JUNG HUN PARK

Estabilização plasmidial através da complementação do gene *icd*^{NAD} e bioprodução de 1,3-propanadiol em *Escherichia coli* recombinante

Dissertação apresentada ao Programa de Pós-graduação em Microbiologia do Instituto de Ciências Biomédicas da Universidade de São Paulo, para obtenção do Título de Mestre em Microbiologia.

São Paulo

2020

JUNG HUN PARK

Plasmid stabilization by *icd*^{NAD} gene complementation and bioproduction of 1,3-propanediol in recombinant *Escherichia coli*

Dissertação apresentada ao Programa de Pós-graduação em Microbiologia do Instituto de Ciências Biomédicas da Universidade de São Paulo, para obtenção do Título de Mestre em Microbiologia.

São Paulo

2020

JUNG HUN PARK

Estabilização plasmidial através da complementação do gene *icd*^{NAD} e bioprodução de 1,3-propanadiol em *Escherichia coli* recombinante

Dissertação apresentada ao Programa de Pós-graduação em Microbiologia do Instituto de Ciências Biomédicas da Universidade de São Paulo, para obtenção do Título de Mestre em Microbiologia.

Área de concentração: Microbiologia

Orientador: Prof. Dr. José Gregório Cabrera Gomez

Versão original

São Paulo

2020

CATALOGAÇÃO NA PUBLICAÇÃO (CIP)
Serviço de Biblioteca e informação Biomédica
do Instituto de Ciências Biomédicas da Universidade de São Paulo

Ficha Catalográfica elaborada pelo(a) autor(a)

Park, Jung Hun
Estabilização plasmidial através da complementação do gene icdNAD e bioprodução de 1,3-propanadiol em Escherichia coli recombinante / Jung Hun Park; orientador José Gregório Cabrera Gomez. -- São Paulo, 2020.
51 p.

Dissertação (Mestrado)) -- Universidade de São Paulo, Instituto de Ciências Biomédicas.

1. 1,3-propanodiol. 2. NADH. 3. Estabilização plasmidial. 4. Escherichia coli. 5. icd . I. Gomez, José Gregório Cabrera, orientador. II. Título.

UNIVERSIDADE DE SÃO PAULO
INSTITUTO DE CIÊNCIAS BIOMÉDICAS

Candidato (a): Jung Hun Park
Titulo da Dissertação: Estabilização plasmidial através da complementação do gene *icd*^{NAD} e bioprodução de 1,3-propanodiol em *Escherichia coli* recombinante.

Orientador (a): José Gregório Cabrera Gomez
A Comissão Julgadora dos trabalhos de Defesa da Dissertação de Mestrado/Tese de Doutorado, em sessão publica realizada a **...../...../.....**, considerou o(a) candidato(a):

( ) Aprovado(a) ( ) Reprovado(a)

Examinador (a): Assinatura: .....

Nome: .....

Instituição: .....

Examinador (a): Assinatura: .....

Nome: .....

Instituição: .....

Examinador (a): Assinatura: .....

Nome: .....

Instituição: .....

Presidente: Assinatura: .....

Nome: .....

Instituição: .....

ICB USP

Cidade Universitária "Armando de Salles Oliveira", Butantã, São Paulo, SP · Av. Professor Lineu Prestes, 2415 - ICB III - 05508 000
Comissão de Ética em Pesquisa - Telefone (11) 3091-7733 - e-mail: cep@icb.usp.br

CERTIFICADO DE ISENÇÃO

Certificamos que o Protocolo CEP-ICB nº **904/2017** referente ao projeto intitulado: ***"Estudo da produção de 1,3-propanodiol em biorreator e a sua relação com a disponibilidade de oxigênio dissolvido no meio"*** sob a responsabilidade de ***Jung Hun Park*** e orientação do(a) Prof.(a) Dr.(a) ***José Gregório Cabrera Gomez,*** do Departamento de Microbiologia, foi analisado pela **CEUA** - Comissão de Ética no Uso de Animais e pelo **CEPSH** – Comitê de Ética em Pesquisa com Seres Humanos, tendo sido deliberado que o referido projeto não utilizará animais que estejam sob a égide da Lei nº 11.794, de 8 de outubro de 2008, nem envolverá procedimentos regulados pela Resolução CONEP nº 466 de 2012.

São Paulo, 21 de agosto de 2017.

Profa. Dra. **Luciane Valéria Sita**
Coordenadora CEUA ICB/USP

Profa. Dra. **Camila Squarzoni Dale**
Coordenadora CEPSH ICB/USP

ICB USP

Cidade Universitária "Armando de Salles Oliveira", Butantã, São Paulo, SP - Av. Professor Lineu Prestes, 2415 - ICB III - 05508 000
Comissão de Ética no Uso de Animais - Telefone (11) 3091-7733 - e-mail: cep@icb.usp.br

Decl. CEPSH.03.2019

DECLARAÇÃO

Em adendo ao Certificado de Isenção CEP **nº 904/2017**, aprovado em 21/08/2017, e por solicitação do Prof. Dr. **José Gregório Cabrera Gomez**, do departamento de Microbiologia, informo que o título do projeto do aluno **Jung Hun Park** foi alterado para ***"Estabilização plasmidial através da complementação do gene icd^{NAD} e bioprodução de 1,3-propanodiol em Escherichia coli recombinante"***, devido às adequações que o projeto sofreu durante o seu desenvolvimento.

São Paulo, 09 de dezembro de 2019.

Profa. Dra. **Camila Squarzoni Dale**
Coordenadora da CEPSH-ICB/USP

Profa. Dra. **Luciane Valéria Sita**
Coordenadora CEUA-ICB/USP

This study was financed in part by the Coordenação de Aperfeiçoamento de Pessoal de Nível Superior - Brasil (CAPES) - processo 88882.333032/2019-01

RESUMO

Park JH. Estabilização plasmidial através da complementação do gene *icd*^{NAD} e bioprodução de 1,3-propanodiol em *Escherichia coli* recombinante. [Dissertação (Mestrado em Microbiologia)] – Instituto de Ciências Biomédicas, Universidade de São Paulo; 2020.

O 1,3-propanodiol (1,3-PDO) é um componente primário para a produção de biopolímeros de alto valor agregado. Este composto pode ser produzido por algumas bactérias em microaerobiose, utilizando glicerol como fonte de carbono. Em um projeto anterior do Laboratório de Bioprodutos, uma cepa de *Escherichia coli* MG1655 foi transformada com um plasmídeo de produção (pBBR1MCS2 :: *dha*) contendo genes de *K. pneumoniae* (operon *dha*) necessários para a conversão de glicerol em 1,3-PDO. No entanto, este plasmídeo é mantido através do uso da canamicina ao meio de cultura, resultando em custos adicionais e questões de biossegurança que podem afetar a produção em larga escala. Para superar este problema, foi proposta uma estratégia de complementação do gene *icd* para estabilizar o plasmídeo de produção, sem a necessidade de antibióticos. O gene codifica uma Isocitrato desidrogenase NAD-dependente e é essencial para o crescimento da bactéria em meio mínimo.

Este projeto teve como objetivo construir uma cepa de *E. coli* com o gene *icd* deletado em seu cromossomo, mas complementada com o mesmo gene no plasmídeo de produção.

A cepa complementada com *icd*$^{NAD}_{(pJ23100)}$ foi testada no ensaio de frasco agitado e a produção de 1,3-PDO sem antibiótico mostrou resultados promissores, produzindo a mesma quantidade de produto que a cepa de controle cultivada com antibiótico. No ensaio de biorreator, a cepa apresentou um fenótipo incomum, no qual a cultura morria ao adicionar anti-espumante e o oxigênio dissolvido (DO) no meio cair repentinamente. Apesar deste problema, uma solução foi encontrada diminuindo gradualmente a DO para atingir a microaerobiose. O rendimento de 1,3-PDO pela cepa complementada por *icd*$^{NAD}_{(pJ23100)}$, sem antibiótico, foi comparável à cepa controle sem a complementação genética usando antibiótico. Apesar disso, foi detectada uma considerável perda de plasmídeo na população de bactérias utilizando a estratégia de complementação gênica. Portanto, uma combinação com um outro sistema de estabilização poderia aumentar ainda mais a produção de 1,3-PDO. Acredita-se que a morte da cultura de células no biorreator esteja relacionada ao aumento da produção de NADH, promovida pela super-expressão do gene *icd*^{NAD}.

Palavras-chave: 1,3-propanodiol. *icd*. NADH. Estabilização plasmidial. *Escherichia coli*

ABSTRACT

Park JH. Plasmid stabilization by icdNAD gene complementation and bioproduction of 1,3-propanediol in recombinant Escherichia coli. [Dissertation (Master thesis in Microbiology)] – Instituto de Ciências Biomédicas, Universidade de São Paulo; 2020.

1,3-propanediol (1,3-PDO) is a primary component for the production of high added value biopolymers. This compound can be produced by some bacteria in microaerobiosis, using glycerol as a carbon source. In the previous project in our laboratory, an *Escherichia coli* MG1655 strain was transformed with a production plasmid (pBBR1MCS2::*dha*) containing *K. pneumoniae* genes (operon *dha*) necessary for the conversion of glycerol to 1,3-PDO. However, the plasmid is maintained by adding kanamycin to the medium, resulting in an additional cost and biosafety issues for large-scale production.

To overcome this problem, it was proposed a strategy of *icd* gene complementation to stabilize the production plasmid without the need for antibiotic. The gene codes for a NAD-dependent Isocitrate dehydrogenase and is essential for growth in minimal medium.

This project aimed to construct an *E. coli* strain lacking *icd* in its chromosome, complemented with the same gene in the production plasmid.

The $icd^{NAD}_{(pJ23100)}$ complemented strain was tested in shake flask assay and the production of 1,3-PDO without antibiotic showed promising results, yielding the same amount of product as the control strain cultivated with antibiotic. In the bioreactor assay, the strain showed an unusual phenotype, in which the culture died when anti-foam was added and Dissolved Oxygen (DO) in the medium suddenly dropped. Despites of this problem, a solution was found by gradually decreasing the DO in order to achieve microaerobiosis. The yield of 1,3-PDO by $icd^{NAD}_{(pJ23100)}$ complemented strain, without antibiotic, was comparable to the strain without gene complementation using antibiotic. Despites of that, considerable plasmid loss was detected in gene complementation strategy, therefore a combination with another stabilization system could enhance the 1,3-PDO production even further.

Cell culture death in bioreactor was suggested to be linked to the overproduction of NADH, promoted by $icd^{NAD}_{(pJ23100)}$ overexpression.

Keywords: 1,3-propanediol. *icd*. NADH. Plasmid stabilization. *Escherichia coli*

ABSTRAKT

1,3-Propandiol (1,3-PDO) ist eine Hauptkomponente für die Herstellung von Biopolymeren mit hoher Wertschöpfung. Diese Verbindung kann von einigen Bakterien unter Verwendung von Glycerin als Kohlenstoffquelle hergestellt werden. In dem vorherigen Projekt in unserem Labor wurde ein *Escherichia coli* MG1655-Stamm mit einem Produktionsplasmid (pBBR1 :: *dha*) transformiert, das K. pneumoniae-Gene (Operon *dha*) enthielt, die für die Umwandlung von Glycerin zu 1,3-PDO erforderlich sind. Das Plasmid wird jedoch durch Zugabe von Kanamycin zu dem Medium aufrechterhalten, was zu zusätzlichen Kosten- und Biosicherheitsproblemen bei der Produktion in großem Maßstab führt.

Um dieses Problem zu überwinden, wurde eine Strategie der icd-Genkomplementierung zur Stabilisierung des Produktionsplasmids ohne die Notwendigkeit eines Antibiotikums vorgeschlagen. Das Gen kodiert für eine NAD-abhängige Isocitrat-Dehydrogenase und ist für das Wachstum in Minimalmedium essentiell.

Dieses Projekt zielte darauf ab, einen *E. coli*-Stamm zu konstruieren, dem *icd* im Chromosom fehlt und der mit demselben Gen im Produktionsplasmid pBBR1MCS2 :: *dha* komplementiert ist.

Der mit $icd^{NAD}_{(pJ23100)}$ komplementierte Stamm wurde im Schüttelkolben-Assay getestet und die Herstellung von 1,3-PDO ohne Antibiotikum zeigte vielversprechende Ergebnisse und ergab die gleiche Produktmenge wie der mit Antibiotikum kultivierte Kontrollstamm. Im Bioreaktor-Assay zeigte der Stamm einen ungewöhnlichen Phänotyp, bei dem die Kultur starb, wenn Antischaum zugesetzt wurde und der gelöste Sauerstoff (DO) in dem Medium plötzlich abfiel. Trotz dieses Problems wurde eine Lösung gefunden, indem der DO allmählich verringert wurde, um eine Mikroaerobiose zu erreichen. Die Ausbeute an mit 1,3-PDO durch $icd^{NAD}_{(pJ23100)}$ komplementiertem Stamm ohne Antibiotikum war vergleichbar mit dem Stamm ohne Genkomplementierung unter Verwendung von Antibiotikum. Trotzdem wurde ein beträchtlicher Plasmidverlust in der Genkomplementierungsstrategie festgestellt, weshalb eine Kombination mit einem anderen Stabilisierungssystem die 1,3-PDO-Produktion noch weiter steigern könnte.

Es wurde vermutet, dass der Zellkulturtod im Bioreaktor mit der durch Überexpression von $icd^{NAD}_{(pJ23100)}$ hervorgerufenen Überproduktion von NADH zusammenhängt.

SUMMARY

1 INTRODUCTION

1,3-propanediol (1,3-PDO) is an organic compound that can be used to produce a diverse range of materials, such as adhesive, paints, solvent, cosmetics and lubricant, but its main usage has been directed to the production of polymers, namely Polytrimethylene terephthalate (PTT) (1–3). This polyester is formed by a transesterefication reaction between 1,3-PDO and terephthalic acid. PTT has an improved elasticity, higher durability and stain resistance, making it attractive for manufacturing of noble grade material such as synthetic carpet, textile fibers, and thermoplastics for engineering purpose (4,5).

1,3-PDO can be produced by chemical synthesis using petroleum-based source. However, with the increasing demand for this polymer and the rising awareness for sustainable production, the industrial biotechnology has emerged as an alternative method, using microorganisms to produce 1,3-PDO (3,6).

Due to the constant evolution of increasingly efficient biological processes and the use of glycerol as a carbon source, the production of 1,3-PDO by biotechnological approach has an economic potential in the market. Gylcerol is a renewable source, produced as a secondary product from the biodiesel industry. Over the years, with the consolidation of biodiesel fuel in the market, the supply of crude glycerol has also increased, resulting in a dramatic drop of its price (7). Lastly, the surplus and lower added value of glycerol have attracted researches encouraging the use of this carbon source as a raw material in the bioindustry, including 1,3-PDO production (8).

1.1 From glycerol to 1,3-propanediol

The metabolic branch of 1,3-PDO is better described in bacteria, such as *Klebsiella pneumoniae*, *Citrobacter freundii* and *Clostridium butyricum*, which contains the necessary genes clustered in an operon (9,10). In the case of *K. pneumoniae* for example, the *dha* operon is composed of six characterized genes. *dhaB*, *dhaC* and *dhaE* encode for subunits of Glycerol dehydratase (DhaBCE), an enzyme responsible for converting glycerol to 3-hydroxypropionaldehyde (3-HPA). This process inactivates DhaBCE, and another enzyme (DhaGF) plus vitamin B_{12} is needed for its recovery to the active form. In the next metabolic step, 1,3-propanediol oxidoreductase (DhaT)

plus NADH (Nicotinamide Adenine Dinucleotide [reduced]) converts 3-HPA to 1,3-propanediol (Figure 1) (11–13).

The production of 1,3-PDO is done by a reducing pathway, while the oxidative pathway of glycerol consumption is related to the production of energy, metabolites and reducing equivalents (NADH and NADPH), necessary for biosynthesis and for the production of 1,3-PDO itself. The equilibrium between the both paths is, therefore, crucial for an efficient production.

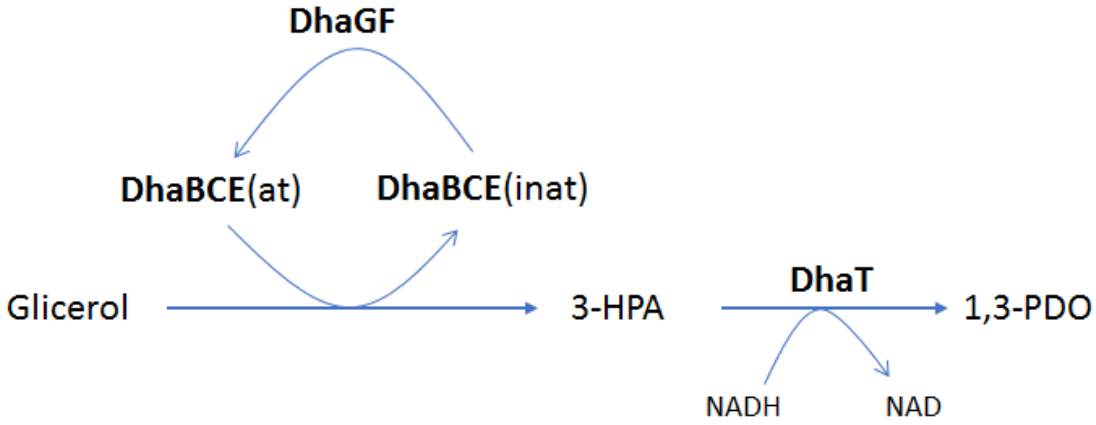

Figure 1: 1,3-propanediol generation from glycerol. Glycerol dehydratase (DhaBCE) depends on DhaGF and coenzyme B12 for regeneration to its active form. 3-hydroxypropanoaldehyde (3-HPA) is reduced to 1,3-propanediol (1,3-PDO) by NADH-dependent enzyme 1,3-propanediol oxidoreductase (DhaT) (11).

The production of 1,3-PDO is also described to be improved under microaerobiosis (14). In this scenario, key regulators of the central metabolism, such as Arc system and FNR, are activated to modulate the transition of the metabolism to a microaerobic condition. As the oxygen concentration is low, less NADH is used in the respiratory chain, resulting in a surplus of NADH that can be directed to 1,3-PDO production (15). However, during this condition, NADH can also be used for the formation of byproducts that might be important for NAD regeneration and maintenance of a proper redox balance in the cell. ArcA and FNR can also positively regulate genes such as *poxB* and *pfl*, that decreases the level of NAD reduction by preventing the carbon flow through NADH generating pathways.

Aiming to prevent the loss of NADH to undesireble byproducts, deletion of genes related to the formation of organic acids is recurrent. In the same way, overexpression of NADH generating enzymes or even *arcA* deletion are also reported to increase the amount of 1,3-PDO (16–20).

1.2 Redox ratio (NADH/NAD) and the central metabolism regulation.

The proper control of the cell metabolism is very important to cell adaptation against environmental changes. ArcAB and FNR systems are the major regulators of *E. coli* metabolic shift between aerobic, microaerobic and anaerobic condition (21). It modulates the expression of many genes from the central metabolism, coordinating the metabolic flux in order to respond rapidly to changes in oxygen availability (22).

The Arc (aerobic respiration control) system is composed of two elements: ArcA, which upon phosphorilation is resposible for regulating the expression of various genes; and ArcB, a membrane redox-sensing protein (23). In microaerobiosis, ArcB is autophosphorilated and transfers its phosphate group to ArcA (ArcA-P) (24,25). Active ArcA-P represses the expression of TCA cycle and glyoxylate shunt related genes. On the other hand, the operon from pyruvate formate lyase catabolic brach (*pfl*) is up-regulated (26). In the respiratory chain, the cytochrome bo operon (*cyoABCDE*) is repressed, while cytochrome bd (*cydAB*) is activated (27–29). This modulation on cytochrome expression in very important, because cytochrome bd has higher affinity to oxygen compared to cytochrome bo, making it more suitable during microaerobiosis, since the oxygen concentration is very low in this scenario (30). *cydAB* activation is also suggested to provide an optimal intracelular environment, by rapidly reducing the available oxygen to H_2O. Oxygen-free cytoplasmic environment is essential for the proper functioning of Pyruvate formate lyase (PFL), because this enzyme, when active, irreversibly reacts to oxygen and loose its function (31). Therefore, once cytochrome bd expression is activated, the flux of pyruvate can now be directed to PFL (32).

FNR is also responsible for regulating essential genes for metabolic shift. The regulator is activated in microaerobiosis, but it is only fully active during anaerobiosis (32). FNR also takes place in repressing TCA cycle genes and activating fermentation related enzymes, but represses both *cyoABCDE* and *cydAB* expression (33).

The shift from aerobic environment to microaerobiosis needs a coordination between ArcA and FNR activation, which ultimately will block TCA cycle and activate Acetil-CoA generation via PFL. The success of this transition also depends on other genes, such as *cydAB* for maintaining a suitable micro-environment and the proper functioning of these enzymes.

NADH/NAD ratio is related to *E. coli*'s central metabolism regulation, as ArcBA and FNR regulated pathways seem to be indirectly activated due to higher redox ratio in the cell (23,29,34–36).

There is also a correlation between NADH/NAD balance and whether the metabolism is directed towards respiration or fermentation. For example, a NADH/NAD ratio about 0.75 is found during anaerobiosis, and 0.02 in fully aerobic environment (32). The ratio is lower in aerobiosis because most of NADH produced is also consumed in the respiratory chain, highlighting the role of respiratory chain in maintaining the redox state lower. It is suggested that these redox ratios are ideal for the proper functioning of the metabolism in different conditions of oxygen availability.

1.3 1,3-PDO production by a recombinant *Escherichia coli*.

The use of *Klebsiella pneumoniae* is not of interest to the industry since it is pathogenic and produce secondary compounds that hampers the purification of the product of interest (37). On top of that, *K*. *pneumoniae* has not been extensively studied, making it more difficult to enhance the productivity by studying its metabolism and genetic modifications (8). To solve these problems several research groups, have cloned the *dha* operon and expressed in a recombinant *E. coli*. Since then, 1,3-PDO production was extensively studied and progress has been made by optimization and genetic modifications in this strain (38–40). A previous project in our laboratory also sought to construct a recombinant *E. coli* harboring the necessary genes for 1,3-PDO production. Firstly, the *dha* operon from *K. pneumoniae* was cloned into pBBR1MCS2 plasmid, resulting in pBBR1::*dha* (plasmid map in Appendix A). This production plasmid was then used to transform *Escherichia coli* MG1655, which was confirmed to be able to produce of 1,3-propanediol (19).

Further modifications in this recombinant strain were also made. In order to increase NADH availability and enhance the production, the wild type *icd* gene (*icd*^{NADP}), which codes for a NADP-dependent Isocitrate dehydrogenase, was substituted to a NAD-dependent icd (*icd*^{NAD}). The production of 1,3-PDO after this modification has increased significantly, confirming the importance of NADH availability. Furthermore, the impact of oxygen supply on 1,3-PDO production in this strain was also studied. The results showed that lower supply of oxygen was beneficial for the production, as described in the literature (19).

The last modification in this strain was the deletion of the *yqhD* gene. It codes for a NADPH dependent-alcohol dehydrogenase that shares a similar function as DhaT, converting 3-HPA to 1,3-PDO (41,42). Metabolic models indicated that YqhD activity is harmful for the synthesis of the product, since it drains NADPH for the synthesis of 1,3-PDO in detriment of cell biomass biosynthesis and even other activities in which NADPH is needed, such as to deal with oxidative stress. Therefore, the deletion of *yqhD* resulted in a higher synthesis of 1,3-PDO from glycerol. (20).
Until this moment the strain *E. coli* MG1655^{NAD} Δ*yqhD* harboring pBBR1::*dha* had the best production of 1,3-PDO in our laboratory.

1.4 Antibiotic-free plasmid stabilization.

E. coli is the most used bacterial chassis in biotechnology. In 2009, almost 30% of protein based recombinant pharmaceuticals were obtained by *E. coli* (43). The production of these compounds is done by heterologous expressions from the genes of interest, and the simplest way of inserting this desirable DNA fragment in the cell is through plasmids. However, keeping these plasmids stable in the bacteria through generations needs a strong selective pressure favoring the cells with plasmid, such as antibiotics in the medium associated to a resistance gene in the plasmid.

Although the use of antibiotics is sufficient to maintain the vector, it leads to an increased production cost, requires purification from the compound of interest, and treatment of the product and the biological waste carrying the gene of resistance. Bioproducts with lower added value that can be alternatively produced by chemical industry are more sensitive to this increase of cost.

Moreover, the emergence of resistant bacteria against antibiotics in the last decades have concerned health agencies and global organizations (FDA, EMEA and WHO) that are recommending increasing limitations in the use of antibiotics and genetic elements carrying antibiotic resistance. In the near future, it is likely that these limitations will become even more restrictive to the industries (44).

Therefore, in order to continue delivering the transition to a more sustainable way of production, it is necessary to find alternatives to reduce the cost of production and to explore alternative ways to stabilize the plasmid.
Fortunately, there are several different strategies to achieve plasmid stabilization without antibiotics. Examples are:

- Operator-Repressor Titration: an essential chromosomal gene is modified by putting its expression under the control of a *lac* operator/promoter. The expression of this gene is blocked, unless IPTG is added. However, in the presence of a multicopy plasmid also containing the *lac* operator, LacI repressor is titrated by the operators in the plasmid, allowing the expression of the essential gene and promoting cell growth (45).
- ParABS system: it allows plasmids to segregate equally to each of its daughter cells, increasing the percentage of the population harbouring the vector. The system consists in two genes *parA* and *parB*, and a sequence called *parS*. In short, ParB specifically recognizes and binds to *parS* site, then ParA interacts to this partition complex to actively segregate the plasmids in a not fully understood ATP-dependent manner (46) (47).
- Toxin-Antitoxin (TA): this method relies on two genes coding for a stable toxin and a less stable antitoxin. The differential decay is essential for the post-segregational killing, whereby the toxin will still be active even after cell division, and daughter cells lacking the plasmid will perish for not being able to replenish the antitoxin (48).
- Gene complementation: an essential gene is deleted from the bacterial chromosome and the same gene is inserted into the desired plasmid. Because the microorganism cannot grow without this gene, daughter cells that end up losing the plasmid will not be able to grow anymore, and thus plasmid borne bacteria are selected. This approach is very commonly used in yeasts (49), and have been successfully used in bacteria as well (50).

1.5 This project

The use of antibiotics in industrial biotechnology has major concerns regarding to the cost and public health safety, which may be impeditive for the production of some bioproducts. In order to address this issue, this project aims to maintain the production plasmid pBBR1::*dha* in *E. coli* without the use of antibiotics, and test the impact of this approach on 1,3-PDO production.

Any of the previously cited strategies for plasmid stabilization could be used for this purpose. However, based on previous findings that increasing NADH results in a higher production of 1,3-PDO, we wondered whether the heterologous overexpression

of *icd*^{NAD} would lead to an even higher production. For this additional purpose, the best strategy is the complementation of *icd* gene, because it is essential for the biosynthesis and *icd*^{NAD} dependent complementation can be used to deliver more NADH to the metabolism.

E. coli Δ*icd* cannot produce α-ketoglutarate, preventing its growth in minimal medium; although supply of glutamate could supplement this limitation (51). In other words, by deleting chromosomal *icd*, only pBBR1::*dha*::*icd* carrying cells would be capable of growing in minimal medium.

As one of the TCA cycle genes, *icd* is down-regulated by ArcA during microaerobiosis. In order to generate more NADH, we also proposed to increase its expression even under low oxygen condition, by simply replacing its native promoter with a constitutive promoter (pJ23100) (52). If correct, this approach should result in an antibiotic free recombinant *E. coli* with an increased capability of production, compared to the previous strain.

Because of ICD's major role in the central metabolism, we did not know whether its overexpression could negatively impact the cell growth. To avoid problems, gradual changes regarding *icd* gene were performed, by first comparing the complementation with icd^{NAD} and icd^{NADP}, and then the impact of using a constitutive promoter.

2 OBJECTIVES

The main goal of this project was to stabilize the production plasmid through *icd* gene complementation and enhance the production of 1,3-PDO at the same time. In order to achieve this goal, it was necessary to:

- Clone *icd*$^{NAD(P)}$ into pBBR1::*dha* plasmid.
- Evaluate the production of 1,3-PDO in *E. coli* Δ*icd* harboring pBBR1::*dha*::*icd*^{NAD} or *icd*^{NADP}
- Test whether production of 1,3-PDO is increased by replacing *icd* natural promoter to a constitutive one.
- Construct a new strain *E. coli* Δ*icd* Δ*yqhD* transformed with the production plasmid complemented with the best variant of *icd* gene
- Perform shake flask and bioreactor assays using this new strain to compare the production of 1,3-PDO with and without kanamycin.

3 MATERIAL & METHODS

3.1 Insertion of different *icd* genes into the production plasmid.

Previous project have already constructed pBBR1::*dha*::icd^{NAD} and *E. coli* Δ*icd*, therefore in this project, we aimed to construct pBBR1::*dha*::$icd^{NAD}_{(pJ23100)}$, pBBR1::*dha*::icd^{NADP} and the double knock-out *E. coli* Δ*icd* Δ*yqhD*.(19)

3.1.1 Amplification of the *icd* gene

Escherichia coli MG1655 and MG1655^{NAD} genomic DNAs were used to amplify the icd^{NADP} and $icd^{NAD}_{(pJ23100)}$ fragment, respectively. pJ23100 constitutive promoter (Anderson et al, 2006) and a Ribosome Binding Site (RBS) site was synthesized along with the primer (synthetic forward), just before the initiation codon sequence. The forward primer (original fw) for icd^{NADP} amplification was designed to anneal at 133 bp before the initiation codon, ensuring amplification of the promoter region of the genome. For both cases, the same reverse primer (icd rv) was used, annealing at 53 bp after the termination codon of the gene. The expected size of the amplicon is 1438 bp for $icd^{NAD}_{(pJ23100)}$ and 1524 bp for icd^{NADP}.

3.1.2 High fidelity PCR of $icd^{NAD}_{(pJ23100)}$ and icd^{NADP}

The amplification reaction was performed using the High-Fidelity Q5 polymerase (New England Biolabs) and the conditions are described below.

PCR conditions were set according to the following parameters:
30 seconds at 98°C, 35 cycles of: 10 sec at 98°C, 15 sec at 65°C, 60 sec at 72°C; and final extra extension of 75 sec at 72°C.

Table 1 – Q5 HF polymerase reaction

Component	Final concentration
5X Q5 Reaction Buffer	1X
dNTPs	200 µM
Forward primer (‘original fw’ or ‘synthetic fw’)	0.5 µM
Reverse Primer (icd rev)	0.5 µM
DNA Template	2 ng
Q5 enzyme	0.02 U/µL

3.1.3 PCR reactions for confirmation purpose

The amplification of the fragments for confirmation of insertion or deletion was performed using the GoTaq Green Master Mix PCR kit (Promega), following its standard procedure.

The primers used for both routine PCR and high-fidelity amplification are described in the table below.

Table 2 – Primer sequences used in this project.

Name	Sequence	Finality
synthetic fw	GGAATTCTTGACGGCTAGCTCAGTCCTAGGT ACAGTGCTAGCTCAATCGCAATAAGGAGGAA ACCACATGGAAAGTAAAGTAGTTGTTCCGG	Forward primer for *icd*$^{NAD}_{(pJ23100)}$ gene amplification
original fw	GGAATTCATCTTTCATGACGGCAAACA	Forward primer for *icd*^{NADP} amplification
icd rv	GGAATTCGATAACCGTTAGCAGCCTAAC	Reverse primer for *icd*$^{NAD}_{(pJ23100)}$ and *icd*^{NADP} amplification
WDconfirmation2R	GTAGAACTACCACCTGACCGGCC	Reverse primer for *icd* deletion confirmation
WDconfirmation1F	GCGAGCTGAATCGCTTAACCTG	Forward primer for *icd* deletion confirmation
EcoR1fw2	TAGGGCGAATTGGAGCTCCA	Forward primer for *icd* insertion confirmation into pBBR1::*dha*
EcoR1rv2	ATAGTGCGACAAGGCTTCCG	Reverse primer for *icd* insertion confirmation into pBBR1::*dha*

ConfDwyqhD	TCCTCCTTTATATGAACTCACC	Reverse primer for *yqhD* deletion confirmation
ConfUpyqhD	CAGAAATGAGCATTGAGAGC	Forward primer for *yqhD* deletion confirmation

3.1.4 Construction of *icd* complemented plasmid production

The amplified insert and the production plasmid pBBR1::*dha* were digested at *Eco*RI restriction site using FasDigest *Eco*RI (ThermoFisher Scientific) following the protocol.

Then, the samples were loaded in agarose gel 0.8% for electrophoresis. The bands indicating the presence of DNA at the size of about 1400 bp for the fragment and 14689 bp for the linearized vector were purified from the gel using Wizard® SV Gel kit and PCR Clean-Up System (Promega). After calculating the vector-amplicon at the ratio 1: 2, the ligation reaction was performed using T4 DNA Ligase (ThermoFisher Scientific) following the protocol.

3.1.5 Transformation by electroporation

Prior to electroporation, it was necessary to make electro-competent cells. For this, the bacteria were previously grown in 20 mL of LB (at 37 °C). In the exponential growth phase OD_{600} = 0.6, the culture was collected and centrifuged at 4900 g for 10 minutes. The supernatant was carefully discarded, and the pellet was washed with MiliQ water (twice) and glycerol solution (10%, v/v), always chilled on ice. Lastly, the cells were resuspended in 100 µL of glycerol (10%), added 1-5 µL of the ligation reaction or plasmid, and electroporated in a 1 mm electroporation cuvette at 1800 Volts.

After the shock, the cells were quickly transferred to a fresh LB medium and incubated under agitation at 37 °C for 1 hour. After the recovery time, the cells were washed and resuspended in 400 µL of 0.85% saline water, then spread on plates containing the selective medium for the transformed cells.

LB agar plates with kanamycin or carbenicillin, or Mineral medium agar plate with kanamycin were used depending on the resistance marker in the plasmid.

3.2 Construction of *E. coli* strain MG1655 Δ*icd* Δ*yqhD*.

In the previous project, Oliveira (2017) constructed an *E. coli* MG1655 ∆*yqhD* :: *kanR* through lambda red technique (20). In this method, the deletion of the gene is done by homologous recombination. For this, primers with homology sequence to the target gene are used to amplify a deletion cassette. The cassette contains kanamycin resistance gene (*kanR*) flanked by FRT (flippase recognition target) regions for future removal of *kanR*, if necessary (53). A lysate of P1 bacteriophage was obtained from *E. coli* ∆*yqhD* :: *kanR* and stocked in the refrigerator.

In this project, the lysate was used for the deletion of *yqhD* in *E. coli* ∆*icd* through transduction. Firstly, the *E. coli* ∆*icd* cells were cultivated in 5 mL of LB liquid medium and, in the exponential growth phase, the cells were washed with $MgSO_4$ (50 mM) and $CaCl_2$ (10 mM) solution. After resuspending them in 1 mL of the same solution, 100 µL of the lysate were added, and incubated at 37 °C. After 30 minutes, 1 ml of LB and 250 µL of 1M sodium citrate were added. After another 30 minutes in agitation at 37 °C, the cells were plated on LB (km) containing sodium citrate (5 mM).

Colonies that grew on the plate were isolated, confirmed by PCR and transformed with the plasmid pCP20. This plasmid contains the gene *flp*, which encodes for a flippase protein necessary for the removal of the kanamycin resistance gene from the deleted *yqhD* region. Transformants with this plasmid were selected on carbenicillin plates and incubated at 30 °C. After confirming the removal of the kanamycin resistance cassette (by PCR), the strain was cured from pCP20 after successive cultures at 37 °C, since the pCP20 has a thermosensitive origin of replication.

3.3 Culture medium

- **Luria-Bertani (LB):** Tryptone (10 g/L), Yeast Extract (5 g/L) e NaCl (5 g/L). For solid medium, Bacto Agar was added to the final concentration of 15 g/L.
- **Mineral Medium:** Na_2HPO_4 (3.5 g/L), KH_2PO_4 (1.5 g/L), $(NH_4)_2SO_4$ (1 g/L), $MgSO_4.7H_2O$ (0.2 g/L); $CaCl_2.2H_2O$ (0.01 g/L), Ferric Ammonium Citrate (0.06 g/L) and Trace elements solution (1 mL/L) [Trace elements composition: H_3BO_3 (0.30 g/L); $CoCl_2.6H_2O$ (0.20 g/L); $ZnSO_4.7H_2O$ (0.10 g/L); $MnCl_2.4H_2O$ (0,03 g/L); $NaMoO_4.2H_2O$ (0.03 g/L); $NiCl_2.6H_2O$ (0.02 g/L); $CuSO_4.5H_2O$ (0.01 g/L)];

agar (15 g/L) for solid medium. The agar and the Mineral Medium solution were separately autoclaved to avoid the formation of precipitation granules. After sterilization, carbon source and necessary elements were added: Glycerol (10 g/L) e vitamin B_{12} (250 µg/L) for shaker flask assays; and Glucose (10 g/L) for solid medium.

When necessary kanamycin at final concentration of 50 µg/mL was added.

- Mineral Medium for Bioreactor: $(NH_4)_2SO_4$ (1 g/L), $MgSO_4.7H_2O$ (0.2 g/L); $CaCl_2.2H_2O$ (0.01 g/L), Ferric Ammonium Citrate (0.06 g/L) and Trace elements solution (2 mL/L) [Trace elements composition: H_3BO_3 (0.30 g/L); $CoCl_2.6H_2O$ (0.20 g/L); $ZnSO_4.7H_2O$ (0.10 g/L); $MnCl_2.4H_2O$ (0.03 g/L); $NaMoO_4.2H_2O$ (0.03 g/L); $NiCl_2.6H_2O$ (0.02 g/L); $CuSO_4.5H_2O$ (0.01 g/L)];

  Glycerol (20 g/L), KH_2PO_4 (1.5 g/L), vitamin B_{12} (250 µg/L), were sterilized separately and added to the mineral medium solution. When necessary, kanamycin (50 ug/mL) and 45 µL of P200 anti-foam were also added. The total volume of medium in the reactor including the inoculum was 3 Liters, unless specified.

  Feeding of glycerol (850 g/L) was done when cultured reached glycerol concentration bellow 8 g/L. Calculation was done to find the amount of glycerol (850 g/L) to be added in order to achieve 20 g/L in the reactor.

$$F = \frac{20 - X}{V}$$

  X = glycerol concentration in the culture (g/L)

  V = predicted total culture volume (L)

  Roughly, glycerol at 850 g/L contains 1g of glycerol per gram of solution. Using a weight balance, add the amount of grams calculated in *F*.

3.4 1,3-PDO production in shake flask assay.

The strains to be tested were previously cultured in LB liquid medium (with kanamycin when necessary) at 37 °C. In the next day, the cells were washed twice with 0.85% saline water. Then, cell density was estimated through 96-wells plate reader spectrophotometer, using the Optical Density (OD) wavelength (600 nm). Before inoculating the bacteria in Mineral medium, a normalization adjustment was

made so that all flasks would receive approximately the same amount of cells, maintaining the final cell concentration at OD_{600} = 0.1.

For the cultivation, 125 mL Erlenmeyer flasks were used, and 50 mL of Mineral medium were added in each flask. The temperature was maintained at 37 °C, with agitation at 150 rpm. The experiments were carried out in triplicate and 1.3 mL of sample was taken every 6 or 12 hours.

Each sample was measured for its OD_{600}, centrifuged and the supernatant was filtered for HPLC analysis. For the plasmid stabilization assay, part of the sample collected was diluted in 0.85% saline solution, in order to obtain Colony Forming Units (CFU) for counting.

3.5 Plasmid stability assay

Samples taken from the shake flask assay were diluted in 0.85% saline water. Dilutions were performed according to the OD_{600} measured on the spectrophotometer, so that the seeding of bacteria resulted between 60 to 150 CFU per plate. Seeding was done in LB and LB (km), and incubated at 30 °C for 18 hours. After counting the CFUs for both plates, plasmid stability was calculated by dividing the CFU from LB (Km) plate by the CFU from LB plate.

3.6 Analytical method (HPLC)

The organic acids, glycerol and 1,3-PDO in the supernatant of shake flasks and bioreactors experiments were measured using High Performance Liquid Chromatography - HPLC (Dionex® ultimate 3000, Thermo Fischer Scientific Inc) equipped with the Aminex-HPX-87H column (BioRad). Glycerol and 1,3-PDO were measured by the refractive index (RI), while organic acids (acetate, lactate, pyruvate, formate, isocitrate and succinate) were measured in the ultraviolet light detector (214 nm). Each injection contained 10 µL of filtered sample and underwent a flow rate of 0.6 mL/min at 40 °C, with 0.05 M sulfuric acid as the mobile phase.

3.7 Pre-inoculum for Bioreactor assay

For the bioreactor assay, a single colony of strains to be tested was picked from the agar plate and inoculated in 20 mL of LB with kanamycin. After 8 hours in agitation at 37 °C, 10 mL of the culture was added to a 1L capacity Erlenmeyer filled with 390 mL of mineral medium (kanamycin and vitamin B_{12} were added) and cultivated for 14 hours. Then, the entire culture was centrifuged, and the pellet was resuspended in 200 mL of 0.85% saline water and inoculated in the reactor.

3.8 Bioreactor specs and aeration control

Dissolving oxygen in liquid is very inefficient. When atmospheric air is used, the maximum capacity of oxygen that can be dissolved in distilled water is 6.99 mgO_2/L at 35 °C (54). When this concentration of saturation is achieved, the dissolved oxygen cannot be increased further by increasing the air flow or the agitation of the culture. The bioreactor's oxygen sensor measures the percentage of oxygen that is dissolved (DO) in the in the culture, being 100% the concentration of saturation for that condition.

In the bioreactor assay, atmospheric air was used to aerate the culture. Bellow the saturation concentration, the stirrer's speed, air flow, pressure in the reactor and foam on the culture can increase the speed of oxygen transfer to the medium, and therefore, the oxygen dissolved increases faster, but the total concentration of dissolved oxygen never surpasses the saturation concentration.

Despites of the increasing consumption of oxygen by a growing population of bacteria in the culture, DO at a specific point, for example 35%, can be maintained by increasing the stirrer speed, so the higher effectiveness of oxygen transfer can compensate the increasing consumption of oxygen.

Both bioreactors used in this project was *Applikon EZ-Control*, with 6 Liters of capacity. Air flow was set to 1 L/min for all the reactor assays.

4 RESULTS

4.1 1,3-PDO production in *icd*^{NAD} and *icd*^{NADP} complemented strain.

icd^{NADP} gene with native promoter was PCR amplified. The insertion of this fragment into the production plasmid was done by standard restriction digestion and ligation, then transformed into *E. coli* Δ*icd*.

The transformed cells were plated in Mineral medium agar plate containing kanamycin, so only *E. coli* Δ*icd* harboring pBBR1::*dha*::*icd*^{NADP} would be capable of growing, although very small colonies without *icd*^{NADP} insertion were also detected. Colony-PCR was done to confirm the presence of the insertion in the plasmid. EcoR1 fw2 and EcoR1 rv2 were used for this purpose (Figure 2).

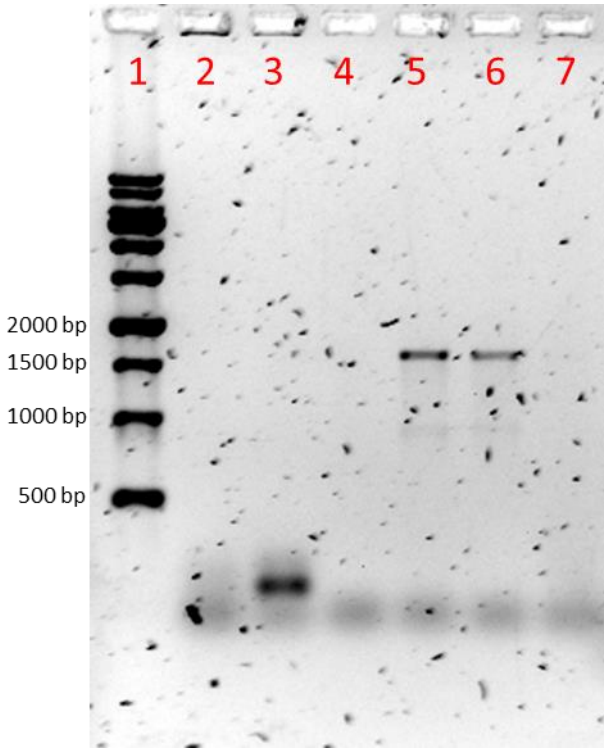

Figure 2: Colony-PCR performed using to detect *E. coli* Δ*icd* + pBBR1::*dha*::*icd*^{NADP}. Successful insertion should give a band of 1670 bp. Lanes: 1 – 1kb ladder (sinapse®); 2 - *E. coli* Δ*icd* (- control); 3 - *E. coli* + pBBR1::*dha* (- control); 4 - MasterMix (- control); 5 to 7 - candidate *E. coli* Δ*icd* + pBBR1::*dha*::*icd*^{NADP}.

One of the positive candidates was isolated and stocked in -80oC ultra freezer. The production plasmid with *icd*^{NAD} gene had already been constructed in the previous project. For the sake of simplicity, *E. coli* Δ*icd* + pBBR1::*dha*::*icd*^{NADP} and *E. coli* Δ*icd* + pBBR1::*dha*::*icd*^{NAD} will be referenced as icdNADP and icdNAD strains, respectively.

For the first comparison, icdNAD and icdNADP, both carrying the natural promoter were subjected to shake flask experiments, in order to test 1,3-PDO production in Mineral medium with and without kanamycin. Figure 3 shows the production of 1,3-PDO from this essay. icdNAD with kanamycin produced 5.60 g/L of 1,3-PDO, and 5.32 g/L in the absence. Comparing this data, we concluded that icdNAD complementation successfully maintains the plasmid without the need for antibiotic. For icdNADP, 1,3-PDO was produced the same amount as icdNAD when kanamycin was added (5.68 g/L). However, without antibiotic, the production decrease drastically (2.07 g/L) (Figure 3). Plasmid stability assay was carried out for this strain, and fast loss of plasmid was detected, explaining the lower production of 1,3-PDO (Appendix B). Because of that, icdNAD strain was chosen to proceed with further experiments.

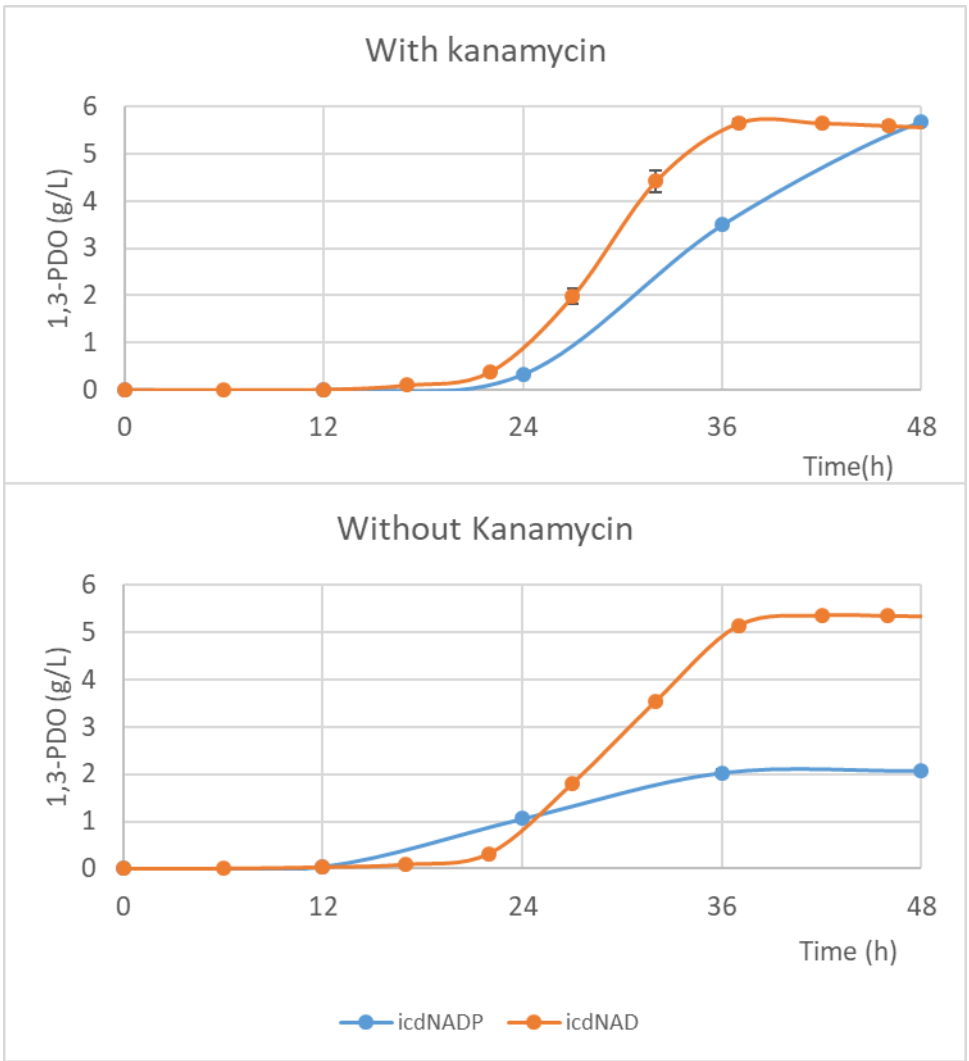

Figure 3: Shake flask assay in Mineral medium comparing the production of 1,3-PDO in *icd*^{NADP} (icdNADP) and *icd*^{NAD} (icdNAD) complemented strains, with and without Kanamycin. The experiment was performed in three replicates and the bar shows the standard error.

4.2 Comparison between *icd*^{NAD} 's natural and constitutive promoter.

icd has its expression negatively regulated in low oxygen concentration. This could decrease 1,3-PDO production as the process occurs mainly in microaerobic condition. In order to circumvent this problem, it was suggested whether a constitutive promoter controlling *icd* expression would increase the production of 1,3-PDO.

To test so, a forward primer harboring a constitutive promoter pJ23100 was used to amplify *icd*^{NAD} gene. The fragment was then inserted into the production plasmid and confirmed by PCR as described before. E coli Δ*icd* + pBBR1::*dha*::*icd*$^{NAD}_{(pJ23100)}$ will be referred as icdNAD(pJ23100).

icdNAD controlled by wild-type promoter or constitutive pJ23100 were compared for the production of 1,3-PDO. The results indicated that icdNAD(pJ23100) produced slightly more 1,3-PDO (5.97 g/L) than icdNAD strain (5.66 g/L). Also, the velocity of production was faster and less biomass (OD_{600}) was needed to achieve these results, with and without antibiotic (Figure 4). Despites of the differences being small, icdNAD(pJ23100) was chosen to proceed with the experiments.

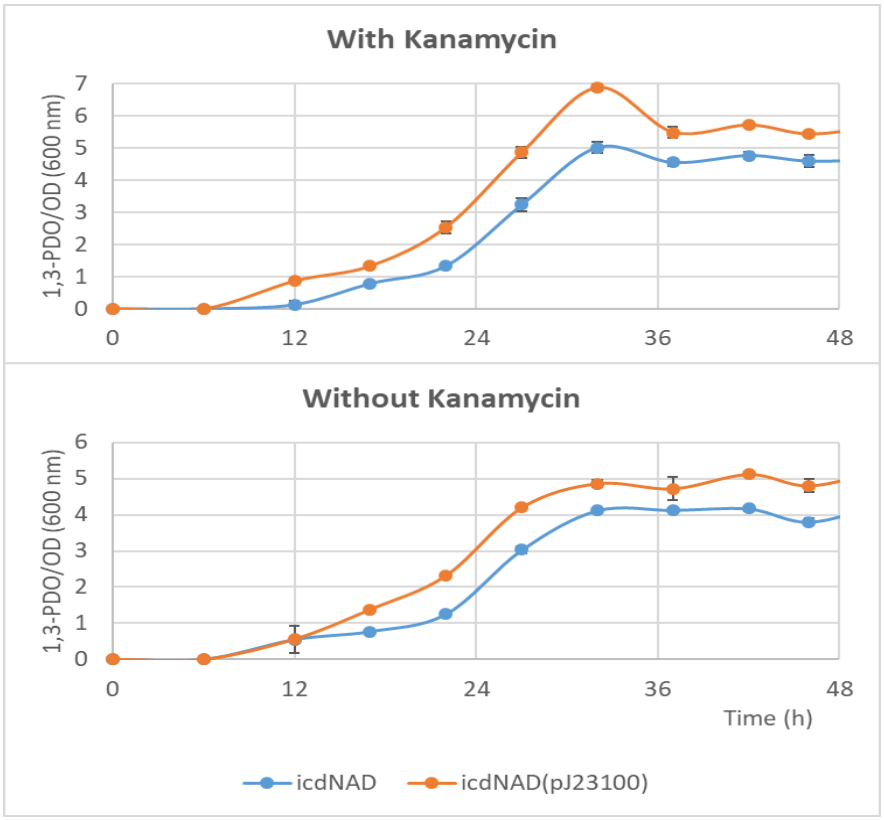

Figure 4: Shake flask assay in Mineral medium comparing the production of 1,3-PDO divided by optical density ($OD^{600\ nm}$) in icdNAD and icdNAD(pJ23100) strains, with and without Kanamycin. The experiment was performed in three replicates and the bar shows the standard error.

4.3 Construction of the definitive strain J2018.

Once the *icd*$^{NAD}_{(pJ23100)}$ complementation was fully tested and showed promising results, the goal was to add this modification to the previous strain *E. coli* MG1655^{NAD} Δ*yqhD* + pBBR1::*dha* and compare the stability of the plasmid with and without this method of stabilization.

To construct such strain, *E. coli* Δ*icd* was picked from the laboratory's strains collection and *yqhD* was deleted through transduction. Figure 5 confirms the deletion of the gene. The double knocked-out mutant was then transformed with the new production plasmid pBBR1::*dha*::*icd*$^{NAD}_{(pJ23100)}$.

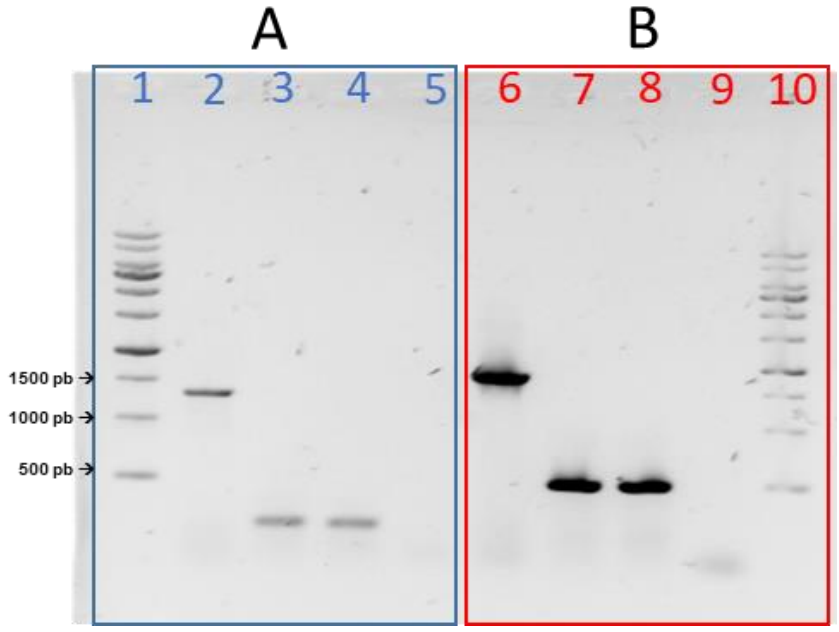

Figure 5: Agar gel showing PCR product using primers flanking the region of *yqhD* (A) and *icd* (B) were used. Lanes: 1 and 10 – Ladder 1kb (sinapse®); 2 – WT (A); 3 – *E. coli* Δ*yqhD* (A); 4 - Candidate *E. coli* Δ*icd* Δ*yqhD* (A); 5 – Negative control (A); 6 - WT (B); 7 – *E. coli* Δ*icd* (B); 8 - Candidate *E. coli* Δ*icd* Δ*yqhD* (B); 9 – Negative control (B). Lower bands from candidate samples that match their respective mutant control indicates that deletion of FRT flaked fragment was successful.

From now on *E. coli* Δ*yqhD* + pBBR1::*dha* and *E. coli* Δ*icd* Δ*yqhD* + pBBR1::dha::icd$^{NAD}_{(pJ23100)}$ will be referenced as H2017 and J2018, respectively. When kanamycin is included in the medium, '(Km)' will be written.

4.4 Shake flask assay for 1,3-PDO production in H2017 and J2018 with/without kanamycin.

One additional shake flask experiment was performed to compare the strain with and without the gene complementation system, in the presence and absence of antibiotic.

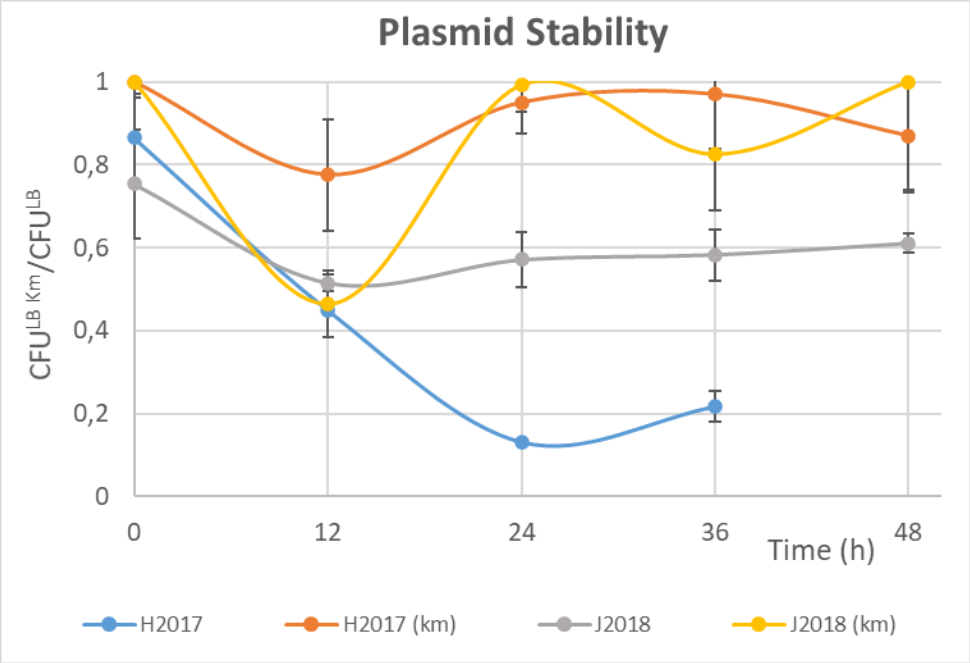

Figure 6: Shake flask assay in Mineral medium comparing the stability of plasmids carried by bacteria. The stability was calculated by the fraction of numbers of colonies that grew in LB with Kanamycin and in LB without antibiotic (CFU $^{LB\ Km}$/ CFU ^{LB}). The experiment was performed in three replicates using H2017 and J2018 strains; the bar shows the standard error.

By comparing the results from H2017 and J2018, it was concluded that gene complementation significantly increases the plasmid stability and consequently the production of 1,3-PDO in the absence of antibiotic (Figure 6 and Figure 7E).

Interestingly, in the absence of kanamycin, J2018 accumulated almost four times more isocitrate in the supernatant (0.160 g/L) compared to H2017 (Km) and J2018 (Km) (0.04 g/L) (Figure 7F). Since J2018 without plasmid is not able to metabolize isocitrate, the accumulation of isocitrate could indicate that some cells are losing plasmids over the time. In fact, plasmid stability assay shows that only 60% of cells are still carrying the plasmid at the end of the assay (Figure 6). Also, J2018 without antibiotic produced slightly less 1,3-PDO (4.60 g/L) compared to the addition of kanamycin (4.86 g/L). Although it means that *icd*^{NAD} complementation strategy is

less efficient than using antibiotic, it does not seem to significantly affect 1,3-PDO formation, quite the opposite, J2018 production is comparable to H2017 (Km) (4.65 g/L) (Figure 7E).

Looking at H2017 without kanamycin, the population carrying plasmids drops rapidly and is followed by a decrease in the pH, and the glycerol consumption stops after 36 hours. Since 1,3-PDO formation regenerates NAD, it is possible that the loss of plasmid resulted in a surplus of NADH. In order to recover the redox balance, the cell increased the production of organic acids and consequently it led to the drop of pH, reaching pH = 4.8 at the end of the experiment; against 6.5 in the presence of Km (Figure 7B). The acetic acid in low pH (4.5 to 5.0) was shown to be inhibitory for *E. coli* O157:H7 (55), explaining the stagnation of glycerol consumption and growth.

As the results were in overall very promising, J2018 was taken to bioreactor assay to test whether this new strain could still produce a reasonable amount of 1,3-PDO without kanamycin.

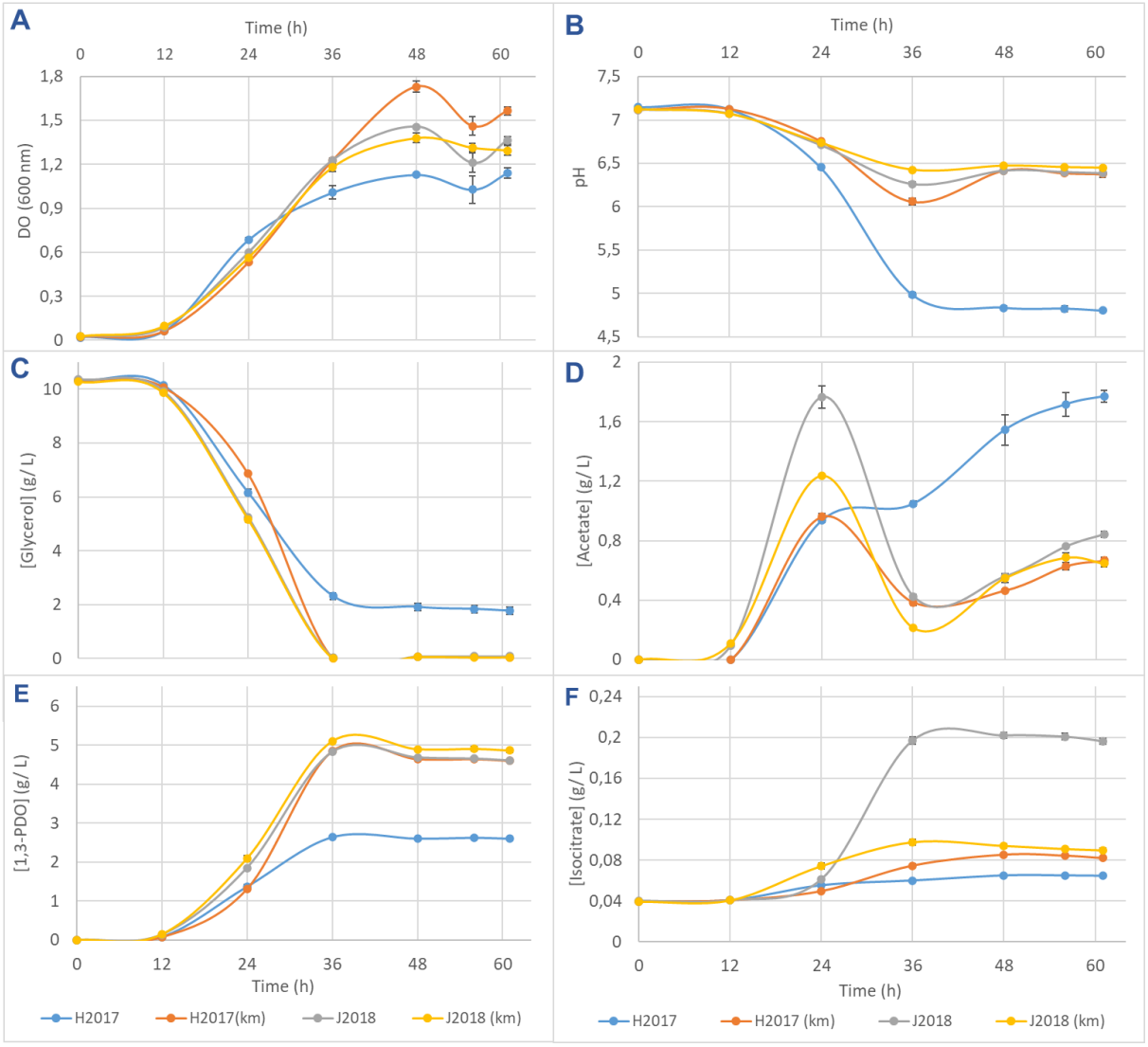

Figure 7: Supernatant of samples were collected for High Performance Liquid Chromatography (HPLC) and pH measurement. The production of organic acids, glycerol consumption and 1,3-PDO production were detected.

4.5 Bioreactor assay comparing H2017 and J2018, with/without kanamycin.

H2017 and J2018 were cultivated in bioreactor, both in the presence of kanamycin. After 10 hours from the inoculation, due to the foam on the medium, the Dissolved Oxygen (DO) stopped to decrease. This is due to the bubbles on the top of the medium, that hold the gases in the liquid and increase the transfer of oxygen to the liquid.

As 1,3-PDO is better produced under microaerobiosis, a DO close to 0% is a more suitable condition. To reach microaerobiosis more quickly, two drops of anti-foam P200 (Propylene glycol) were added to the reactor. From this moment, the DO suddenly dropped and the velocity of 1,3-PDO production started to raise. However, for J2018 (Km), after approximately 2 hours, the DO started to increase, until it

achieved 100% (Figure 8C). This scenario indicates that cells are no longer consuming oxygen. After 4 hours from the time anti-foam was added there was no glycerol consumption and 1,3-PDO formation ceased (Figure 8D and 8A). Dried Cell Weight (DCW) collected from the experiment also showed that cells stopped growing after the addition of anti-foam (Figure 8B). Together, these data suggest that the culture might have died after a couple of hours.

For H2017 (Km), the experiment was successful and 21.13 g of 1,3-PDO and 4.74 g of biomass were produced in the end of the experiment ($Y_{(P/X)}$ = 4.45 g/g).

The bioreactor for J2018 (Km) was repeated, but once again, the culture died after the addition of anti-foam. Then it was proposed that genetic modification in this strain could have resulted in a more sensitive phenotype to the defoamer. So, we increase the period of time for bacterial growth before adding the anti-foam, but it had the same effect and the culture stopped growing.

Then, it was hypothesized that replacing *icd* natural promoter to a constitutive one, could have resulted in the lack of its regulation. Maybe, the overexpression of this gene could be affecting the cell metabolism in this specific condition of transition between aerobic to microaerobic state. To test this hypothesis, *E. coli* Δ*icd* Δ*yqhD* was transformed with the production plasmid complemented with icd^{NAD} carrying the native promoter. The bioreactor was carried out, however the culture kept dying after anti-foam addition. Showing that icd^{NAD} overexpression by multi-copy plasmids was probably enough to lead to this phenotype. In other words, the problem was linked to the strategy of icd^{NAD} complementation.

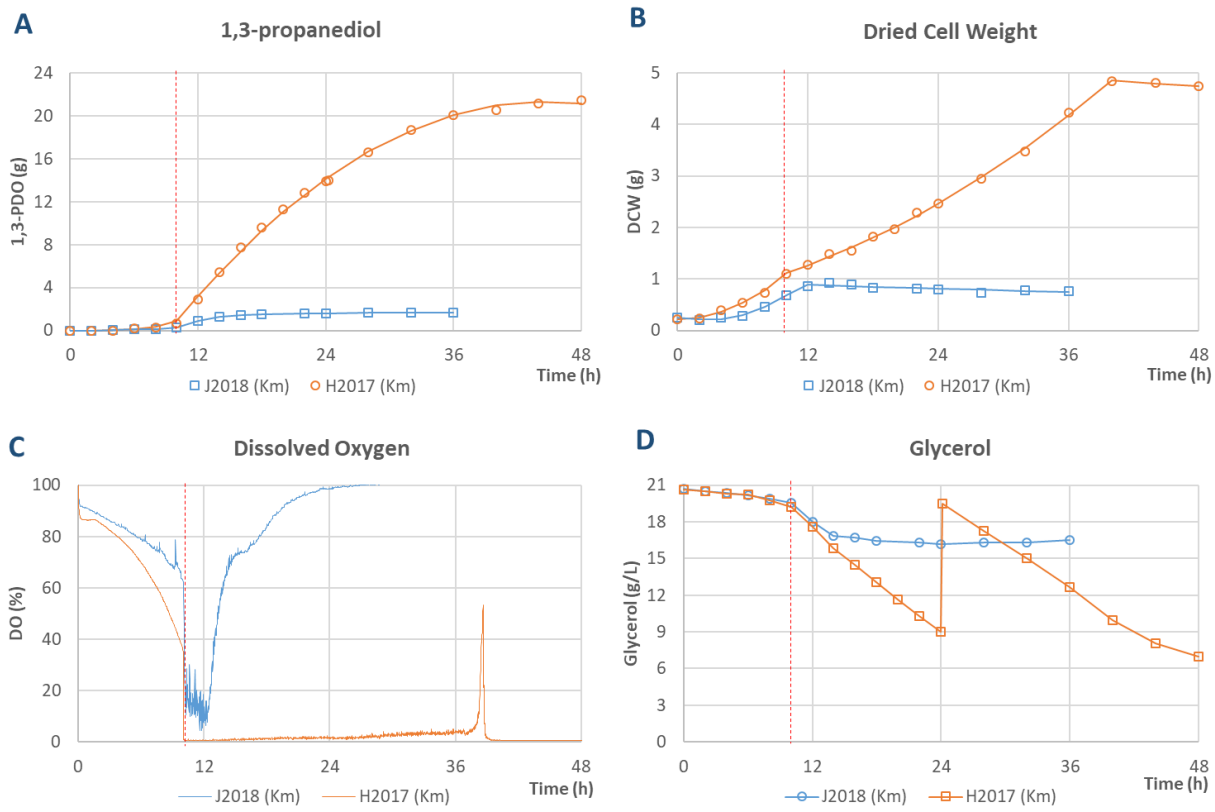

Figure 8: Bioreactor assay in Mineral medium with Kanamycin, comparing H2017 and J2018. Anti-foam was added after 10 hours from the beginning of the experiment (red dotted line). The comparison between the two strains could not be done because J2018 was inhibited or died as shown in (B), (C) and (D). H2017 performed as expected based on the previous project.

Analyzing the oxygen consumption data from these failed assays, it was noticed an unusual pattern after adding the anti-foam: the DO always started to indicate up and down consumption of oxygen, but never reaching to 0% (Figure 8C). Also, after antifoam addition, a peak of pyruvate and acetate was detected (Appendix C). However, it was not clear whether anti-foam was the primary cause of these phenotypes and cell death.

To answer to this question, we performed another bioreactor (total volume = 2 Liters), but this time controlling the DO above 30% (which is a fully aerobic condition) for the entire experiment. During this reactor, several drops of anti-foam were added, and this time, the culture did not die. Therefore, it was clear that anti-foam was not the primary cause of the culture death, but the DO decrease in this modified strain.

The above-mentioned reactor compared 1,3-PDO production with and without kanamycin, and the final amount was the same in both cultures (6,8 g) (Figure 9B). Consistent with the shake flask experiments, the absence of kanamycin resulted in a

higher accumulation of isocitrate (Figure 9D). Interestingly, lactate and high yield of formate were detected (Figure 9E and 9F) which is very unusual for an aerobic assay.

Because of high oxygen supply, the culture grew exponentially during the first 24 hours, achieving about 5.5 g of biomass (Figure 9A). The productivity of 1,3-PDO was very low in this assay ($Y_{(P/X)}$ = 1.23 (g/g)), which is expected because aerobic condition is not proper for 1,3-PDO production. Thus, microaerobiosis have to be achieved for an adequate study of *icd*$^{NAD}_{(pJ23100)}$ complementation.

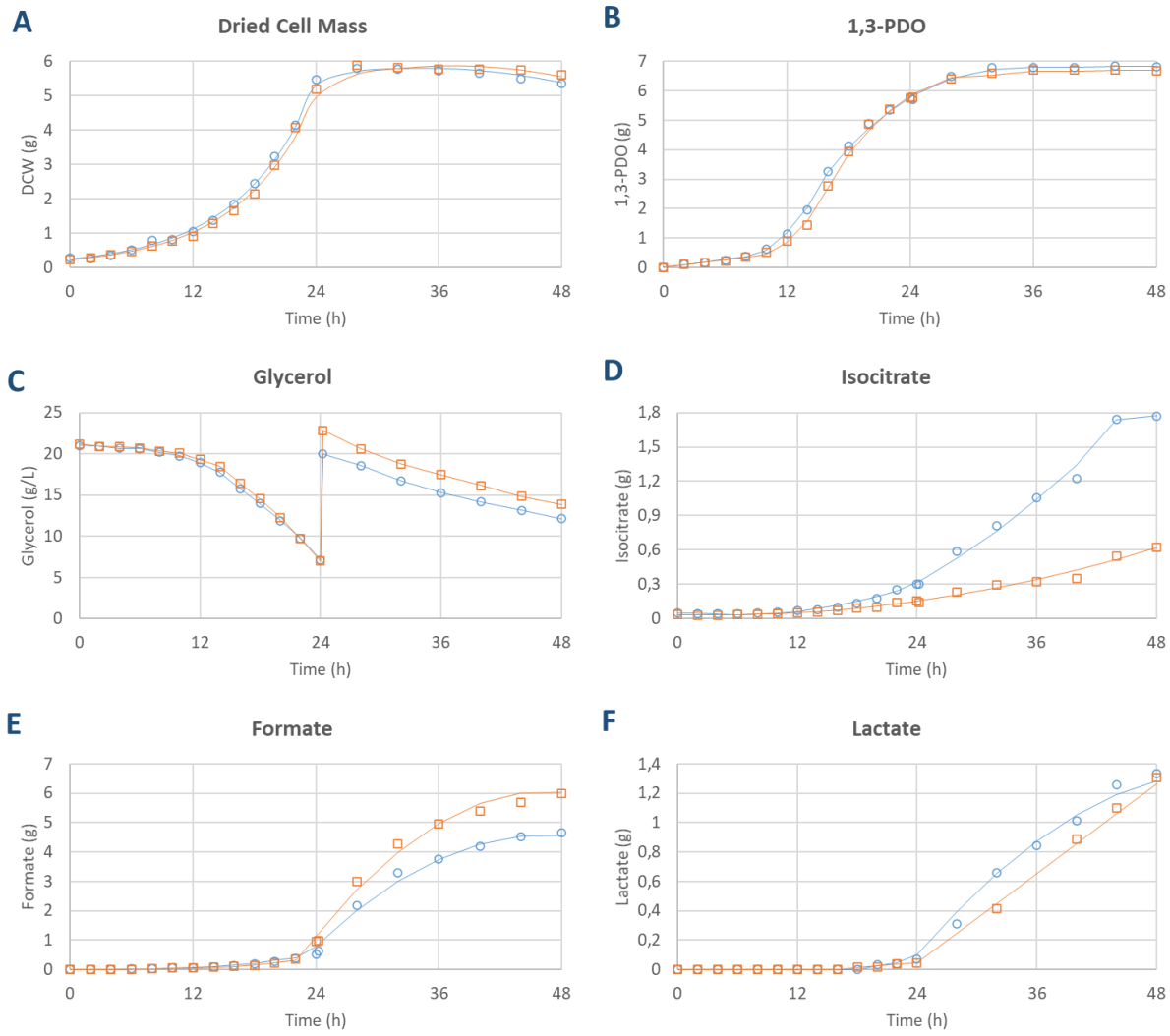

Figure 9: Bioreactor in Mineral medium with and without antibiotic. The experiment was carried out under aerobic condition (DO above 30%) by increasing the stirrer rotation. Several drops of anti-foam were added during the experiment, but no such inhibition of cell death was detected this time. Circle Blue ○: J2018; Square Orange □: J2018 (Km)

Now that anti-foam was discarded as the main cause to cell death, the next step was to test whether DO drop alone could result in this phenotype, or whether it was the addition of anti-foam in this specific condition to microaerobiosis that was the

causing the culture death. However, as the main goal of this project was to assess *icd*$^{NAD}_{(pJ23100)}$ gene complementation, instead of trying to elucidate the reason behind cell death, it was decided to circumvent the problem and not to solve it.

Therefore, based on the premise that cells cultivated in Erlenmeyer gradually go from aerobic condition to microaerobiosis, and based on the observation that culture death never occurred in any of the shaker flask experiments, using this strain. It was concluded that the problem could be related to the **sudden** drop of DO, and therefore, maybe, decreasing DO gradually could prevent this problem to happen.

If the suspicion on the fast drop of DO and cell death was correct, anti-foam could be added before the beginning of the experiment, preventing the formation of bubbles for the first 24 hours and providing gradual decrease of DO.

As a last alternative, this method was carried out adding anti-foam (45uL) before autoclaving the medium in the reactor. In this bioreactor, J2018 was tested in the presence of kanamycin. The DO decreased from 98% in the beginning of the experiment to 0% after 10 hours of cultivation (Figure 10B) and this time, the culture survived, producing 17.56 g of 1,3-PDO and 4.38 g of biomass in 48 hours (Figure 10A) ($Y_{(P/X)}$ = 4 g/ g).

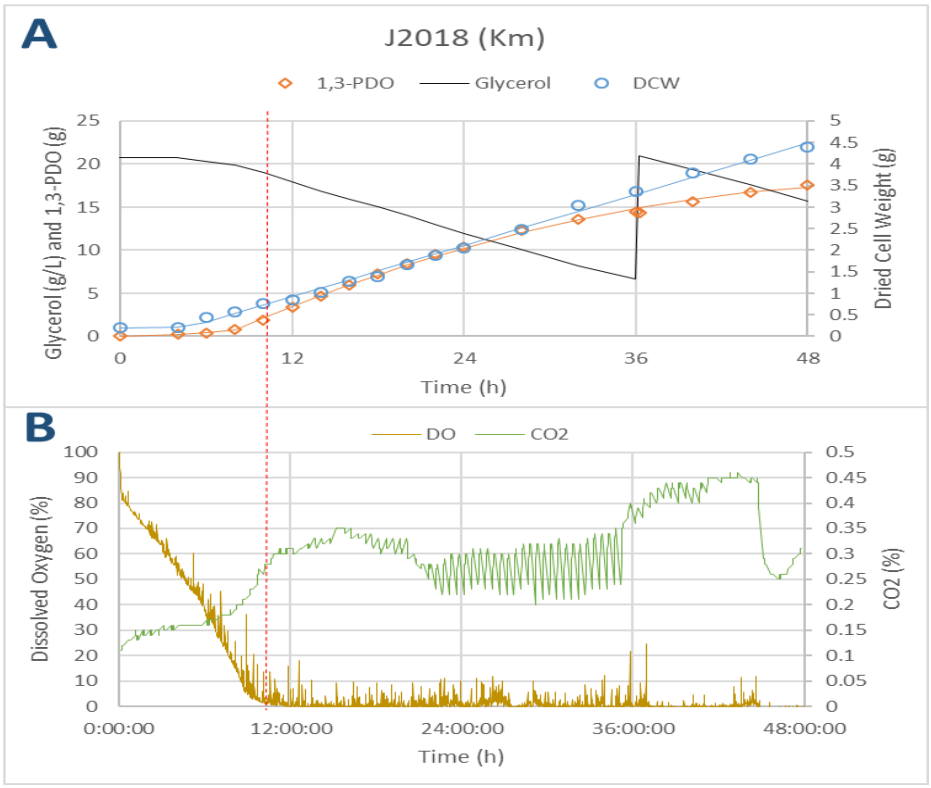

Figure 10: Bioreactor in Mineral medium with Kanamycin. Anti-foam was added before the sterilization to enable gradual decrease of DO. Red dotted line marks the moment that J2018 achieved microaerobiosis in DO close to 0%. (A) – production of 1,3-PDO, cell density (DCW) and concentration of glycerol. (B) – Dissolved oxygen in the medium and CO_2 gas released by the bacteria in the headspace.

Despites of the success, the production of 1,3-PDO was still considerably lower than expected. Analyzing the data, the biomass of this assay was found to be around 0.25 g/L when the DO reached to 0%. Low concentration of bacteria at the beginning of the production phase can lead to lower yield, as the culture growth enters in linear phase when oxygen is limiting. In other words, less biomass will produce lower amount of 1,3-PDO over time.

In order to solve this problem, the following bioreactors had an extended period of time for bacterial growth, where DO was maintained above 35%. To keep good aeration during this time, the reactor's software was programmed to increase the stirrer's speed in order to keep DO above 35% (For better explanation see section 3.8 in Methods). The CO_2 released by the culture was used to indirectly measure the biomass in the reactor, as more bacteria will release more CO_2 through respiration. CO_2 at 0.5% was chosen as a parameter to stop the stirrer's control and start to decrease its rotation, in order to start the production phase (Figure 11). Therefore, when the culture reached the concentration of 0.5%, the stirrer gradually decreased to 200 rpm and kept at this rate until the end of the experiment. DO 0% was achieved as soon as the stirrer started to decrease its rotation.

Following this procedure two bioreactors were performed, comparing J2018 with and without antibiotic. The culture survived and we could finally assess the production of 1,3-PDO under microaerobiosis, comparing *icd*$^{NAD}_{(pJ23100)}$ complemented strain with and without antibiotic. In the presence and absence of kanamycin, the outcome was 30.63 g of 1,3-PDO ($Y_{(P/X)}$ = 6.03), and 21.3 g ($Y_{(P/X)}$ = 4.9 g/ g) respectively.

Later, H2017 was also tested with and without kanamycin, following the same procedure as described before. H2017 (Km) produced 19.48 g of 1,3-PDO ($P_{(P/X)}$) = 4.43), and 12.86 of 1,3-PDO ($P_{(P/X)}$ = 2.16) for H2017.

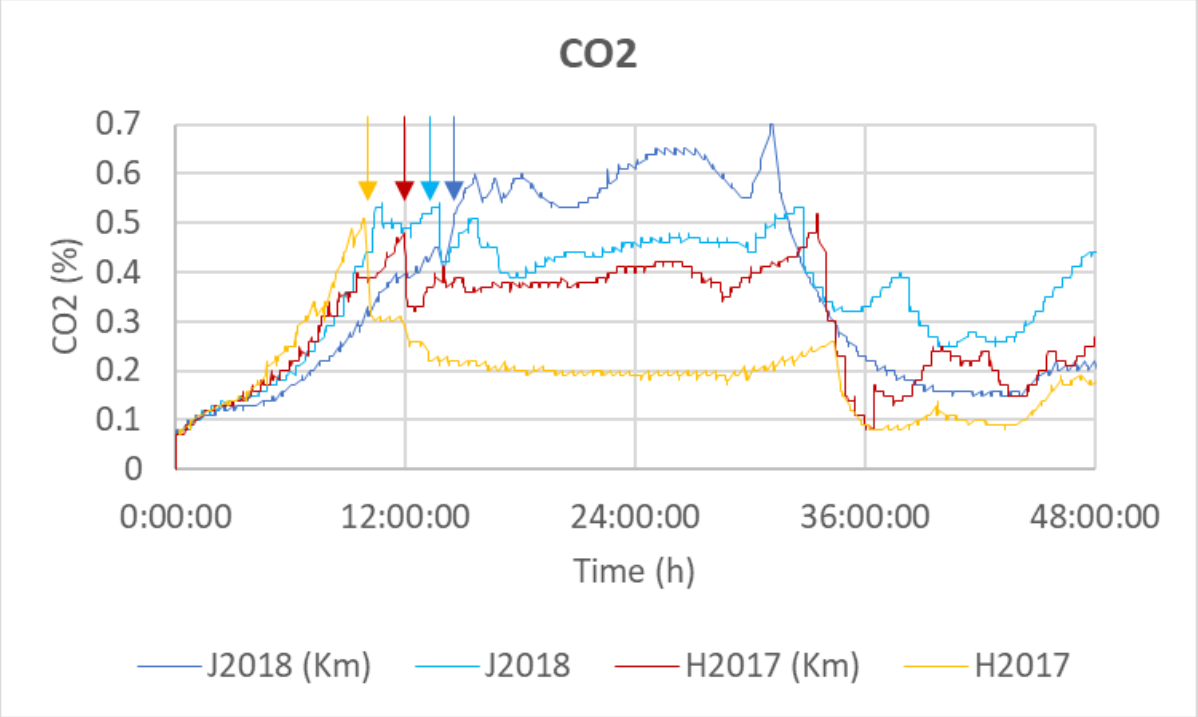

Figure 11: Percentage of CO_2 in the bioreactor's headspace. The arrows of respective color indicate the moment that 0.5% level of CO_2 gas was achieved, shortly thereafter the stirrer was set to gradually decrease to 200 rpm.

At the first glance, *icd*$^{NAD}_{(pJ23100)}$ complementation seems to be considerably inefficient for plasmid stabilization, as J2018 (Km) produced dramatically more 1,3-PDO than J2018 (Figure 12B). However, a closer look at DO and biomass collected from J2018 (Km) shows that the culture did not achieve 0% DO until 32 hours of experiment, and therefore it did not have a linear growth phase. J2018 (Km) could be producing more in fact, and this would be consistent to the results in shaker flasks. However, because of these differences in kinetics, the results from J2018 (Km) are isolated and not comparable to the other experiments.

On the other hand, J2018 and H2017 (Km) had the same pattern of growth and production, showing that *icd*$^{NAD}_{(pJ23100)}$ complementation also works in conditions met in the bioreactor. Isocitrate accumulation was also detected in J2018, once again indicating the possibility of plasmid loss (Figure 12C).

This stabilization system might not be better than using kanamycin, but even then, 1,3-PDO production was not affected compared H2017 (Km) (Figure 12A and 12B). There is a supposition that increased production of 1,3-PDO caused by NADH overproduction compensates the plasmid instability in J2018.

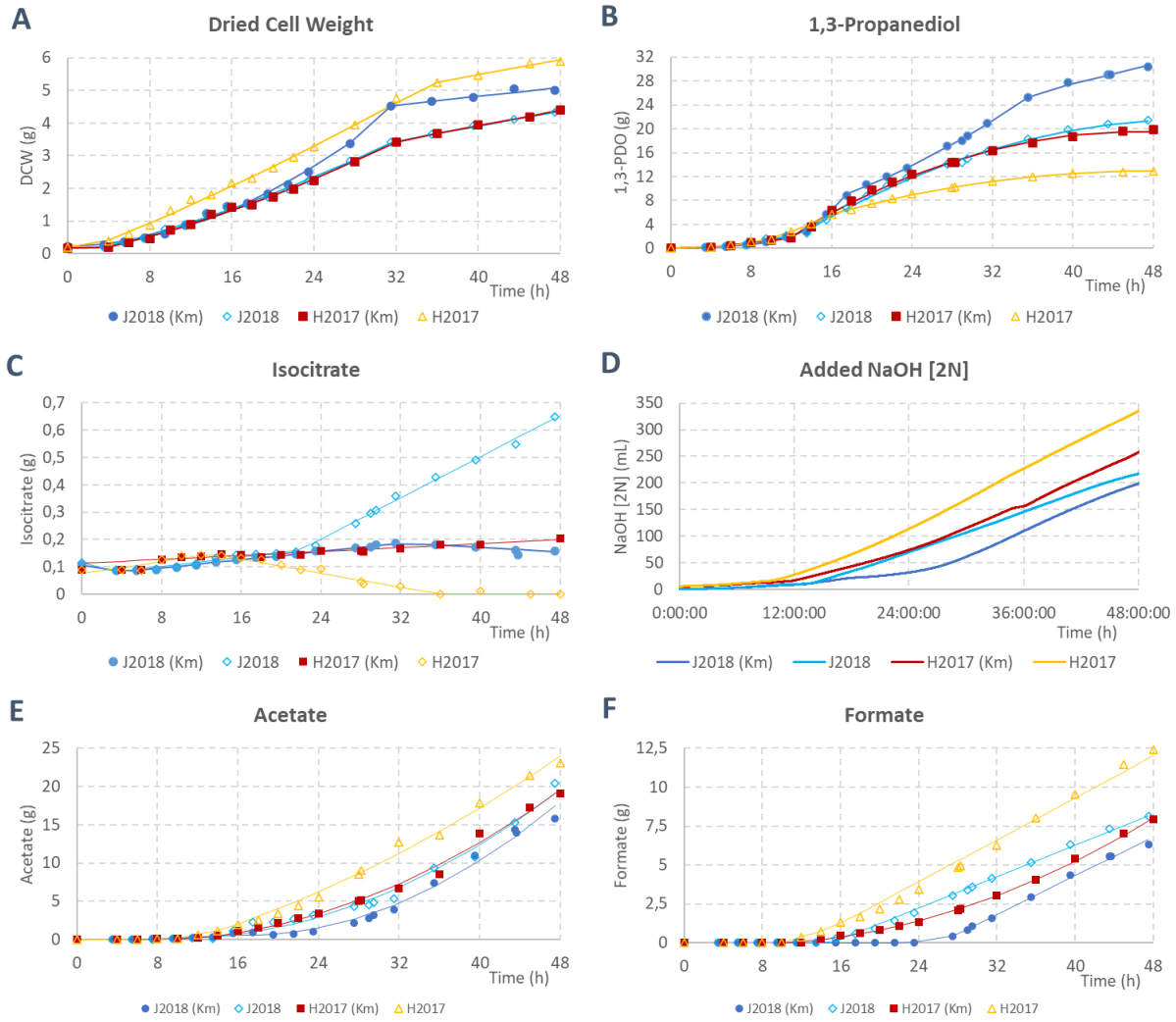

Figure 12: Bioreactor assays performed in Mineral medium, with and without Kanamycin. H2017 and J2018 strains are compared regarding 1,3-PDO production, organic acids and Dried Cell Weight.

In the absence of kanamycin, H2017 performed very poorly, directing most of glycerol to cell growth and to the production of organic acids (Figure 12A, 12E and 12F). This data is consistent to the shake flask assay by showing higher production of organic acids and requiring more addition of NaOH 2N solution to the medium (Figure 12D), in order to maintain pH = 7.0. As pH is controlled in bioreactor, inhibitory event does not happen, thus glycerol consumption and 1,3-PDO generation is continuous until the end of the experiment.

These results are consistent with the experimental data collected from the shaker assay, adding evidence for the partial success of *icd*$^{NAD}_{(pJ23100)}$ gene complementation for plasmid stabilization and 1,3-PDO production.

5 DISCUSSION

5.1 Plasmid stabilization by *icd*$^{NAD(P)}$ complementation.

In contrast to the gene complementation by *icd*^{NAD}, *icd*^{NADP} did not work as expected. The plasmid was lost very quickly in the absence of antibiotic, leading to lower production of 1,3-PDO. When the antibiotic was added, the production was restored to the same level as icdNAD strain, however, there was a significant loss of specific growth and production rate. According to these data, it was hypothesized that *icd*^{NADP}, but not *icd*^{NAD} complementation could have disadvantageous features that could compromise cell growth. In fact, overproduction of NADPH is known to be toxic for cell metabolism, which is represented by slower growth (56,57). NADPH excess could be a problem by depleting NADP and preventing the metabolic flux in steps where this oxidized cofactor is necessary (56), but it is also related to the inhibition of citrate synthase in the TCA cycle (58), which is the major source of energy equivalents during aerobic growth. Depending on the source mutation responsible for NADPH overproduction, normal growth can be restored by increasing the flux for its consumption, either by overexpressing *udhA* or other metabolic branches that utilizes NADPH, such as ethylene-forming enzyme (EFE) and 3-hydroxybutyrate (3-HB) (59–61).

As icdNADP strain lacks this additional source of NADP regeneration, we believe that carrying this plasmid would result in a tremendous burden for the cells to keep with it, and cells that have lost the vector would be naturally selected by growing faster than plasmid-borne cells. This could explain why plasmid loss happens so quickly, but according to our previous knowledge about *icd* knock-out, this would not be possible, as plasmid loss also results in blocked biosynthesis by preventing the formation of α-ketoglutarate.

However, things started to become clear when we found that we have neglected the fact that *E. coli* passively leaks α-ketoglutarate in the medium (62). Although the leaked concentration is very low (1 µM), it was found that upon *kgtP* (α-Ketoglutarate permease gene) deletion, the concentration of α-ketoglutarate increased linearly, in function of OD_{600}, reaching to almost 30 µM at OD_{600} = 0.8 (63). KgtP is responsible for actively importing α-ketoglutarate to the cell (64), and it is suggested to be negatively regulated by ArcA and FNR (65). As previously discussed in the Introduction

section, disturbing redox balance (such as increasing NAD(P)H concentration) might affect the proper functioning of ArcA and FNR regulated genes. Therefore, downregulation of *kgtP* and consequent accumulation of α-ketoglutarate in the medium is likely to happen in icdNADP or icdNAD strains.

In summary, it is possible that icdNADP strain carrying the production plasmid is leaking considerable amount of α-ketoglutarato in the medium, which is a source of nutrient for cells who lost the vector. This provides a condition where the burden for keeping icd^{NADP} complemented plasmid is much higher than becoming dependent on α-ketoglutarate leakage. Plasmid cured cells do not overproduce NADPH, and therefore grow faster and rapidly takes over the population, leading to low 1,3-PDO production. A similar condition could be happening to icdNAD strain as well, but at a lower rate, since NADH overproduction does not seem to significantly affect the cell growth, so maintaining the plasmid should be less disadvantageous. Nevertheless, plasmid loss does occur in icdNAD strain, as shown by the plasmid stability assay in shaker flasks and the increasing amount of isocitrate along all the assays.

Regarding to plasmid stabilization, complementing $icd^{NAD}_{(pJ23100)}$ gene turned out to be partially effective. However, despites of this problem J2018 without Km produced the same amount of 1,3-PDO, comparing to H2017 (Km). On top of that, upon addition of antibiotic in J2018 culture, the production was even higher. This is a very promising result, showing that increasing NADH availability by overexpressing icd^{NAD} does positively impact 1,3-PDO production. It also indicates that there is still room for improvement on plasmid stabilization that could result in a better production of 1,3-PDO, without the use of antibiotics.

A simple solution to enhance J2018's plasmid stabilization is by adding a parABS system. The equal segregation of plasmids should decrease the likelihood and speed of plasmid loss. However, if the proposed option does not work, other stabilization strategies that does not disturb with redox balance might be more suitable for this purpose. For example, stabilization by Toxin-Antitoxin (TA) system has proven to be very efficient for a fed-batch production of a recombinant protein in *E. coli* (66).

5.2 NADH overproduction may lead to the lack of fine control for aerobic to microaerobic metabolism shift.

The increased production of 1-3-PDO by J2018 (Km) over H2017 (Km) can indicate that over-expression of *icd*$^{NAD}_{(pJ23100)}$ gene caused by multi-copy and constitutive promoter resulted in an increased amount of NADH, as planned. However, although higher concentration of NADH is desired for better production, it could also have disturbed the redox balance in the cell.

As presented in the Introduction section, NADH/NAD ratio seems to affect the activation of some of ArcA and FNR regulated genes, so we hypothesized that higher redox ratio would affect the activation of some of these key enzymes responsible for the fermentation metabolism.

Accordingly, when bioreactor was performed maintaining 30% DO, lactate and high concentration of formate was detected, which is unexpected, since these organic acids are produced during fermentation. This might be an evidence that metabolism in this strain is not working properly. Sánchez et. al (67) also reported an *E. coli* strain producing formate in aerobic condition, his strain had an *udhA* overexpression, a transhydrogenase that transfers reducing equivalents from NADPH to NAD, forming NADH + NADP. This overexpression resulted in a lower NADPH/NADP ratio and higher NADH/NAD ratio compared to the wild-type strain. Rivera et. al 2002 (68,69) also aimed to increase NADH availability, and as a consequence, fermentation byproducts were detected despites of growth under aerobic condition. The author suggests that the reduced environment in the cell stimulated the metabolism towards the oxidation of NADH excess through fermentative process, in order to achieve the redox balance. These reports support the hypothesis that NADH overproduction by *icd*^{NAD} complementation might have led to a disorded metabolism and consequently unexpected production of formate and lactate.

If NADH/NAD unbalance does affect the bacterial central metabolism, it is reasonable to hypothesize that cell death after DO sudden drop (by anti-foam addition), is also related to NADH overproduction. One interesting finding in all the bioreactors that have failed, was the detection of pyruvate and sudden increase of acetate in the medium, after the addition of anti-foam. We believe that pyruvate accumulation may indicate blockage of downstream catabolism. As Pyruvate dehydrogenase (PDH) and TCA cycle activities are repressed under microaerobic condition (32,70), the pyruvate

should be channelled to Pyruvate Formate Lyase (PFL). However, since no formate is detected in a reasonable concentration, it is possible that pyruvate is not being directed to PFL either. This could be caused by an overproduction of NADH that leads to a fast activation of ArcA. Consequently, it would result in cytochrome bo (*cyoABCDE*) inactivation and cytochrome bd (*cydAB*) activation, even though the surrounding environment still have a reasonable concentration of oxygen. Without proper consumption of oxygen, PFL pathways cannot take place, explaining pyruvate accumulation. Acetate production can be explained by direct conversion of pyruvate to acetate through PoxB. PoxB is suggested to decrease oxidative stress and seems to have its major role during microaerobiosis, where flux through PDH and PFL are suboptimal (71).

A problem in the respiratory chain can also be evidenced in the majority of bioreactors that resulted in culture death, where the culture was not able to reach 0% DO, although at that cell density, the oxygen should be rapidly consumed and enter in microaerobiosis state, as shown in successful bioreactors. This also supports the hypothesis that *cyoABCDE* is not active, summed to the fact that *cydAB* alone cannot efficiently support aerobic respiration (72).

The reason for succeeding bioreactors through gradual decrease of aeration is unknown. However, based on our results, we can infer that this strain may need more time and less aggressive change in the environment to cope with this stressful shift in the metabolism.

The research in the literature just give us some clues for making hypothesis, but as this phenotype is very specific to the condition imposed by our assay, it is difficult to know what is really happening. To truly understand the mechanism by which the cells are dying and the unexpected behaviour of its metabolism, it is necessary to obtain data about gene expression or metabolic flux, through RT-PCR or RNAseq and carbon labelling focusing on key genes responsible for transitioning from aerobic to microaerobic metabolism. We believe that this data could add more information and help to better understand about this complex metabolic shift to microaerobiosis.

6 CONCLUSIONS

Plasmid stabilization by *icd*^{NADP} complementation turned out to be inefficient for 1,3-PDO production. The overproduction of NADPH and consequently growth inhibition is believed to the main cause for the rapid plasmid loss. On the other hand, *icd*$^{NAD}_{(pJ23100)}$ complementation showed promising results by enhancing plasmid stability without the use of antibiotic. As a result, the strain carrying this complementation system did not require antibiotic and produced the same amount of 1,3-PDO as the strain dependent of antibiotic. However, when antibiotic was added, J2018 produced 63% more (in total grams) of 1,3-PDO than H2017; and in the absence of antibiotic, J2018 produced 60% more than H2017.

icd$^{NAD}_{(pJ23100)}$ complementation does not fully stabilize the production plasmid, as evidenced by isocitrate accumulation and stability assay. However, it opens the possibility that combining this strategy with another stabilization system, might increase 1,3-PDO production even further.

It seems that *icd*^{NAD} overexpression did result in a higher amount of NADH for 1,3-PDO production. Meanwhile, the excess of NADH also affected the central metabolism regulation, causing cell cycle arrest and death upon rapid environmental change from aerobic to microaerobic condition. The actual reason for this phenotype is still unknown, and further studies comprising gene expression and metabolic flux experiments in this strain are needed. The understanding of the cause of this phenotype could add more information about the metabolism in *E. coli*.

REFERENCES*

1. Sauer M. Microbial production of 1, 3-propanediol (Bio-PDO™). 2007;191–7.
2. Cheng KK, Zhang JA, Liu DH, Sun Y, Liu HJ, Yang M De, et al. Pilot-scale production of 1,3-propanediol using Klebsiella pneumoniae. Process Biochem. 2007;42(4):740–4.
3. Zhu MM, Lawman PD, Cameron DC. Improving 1 , 3-Propanediol Production from Glycerol in a Metabolically Engineered Escherichia coli by Reducing Accumulation of sn-Glycerol-3-phosphate. Plasmid. 2002;694–9.
4. Xie Q, Hu X, Hu T, Xiao P, Xu Y, Leffew KW. Polytrimethylene Terephthalate: An Example of an Industrial Polymer Platform Development in China. Macromol React Eng. 2015;9(5):401–8.
5. Silva GP da, Contiero J, Ávila Neto PM, Lima CJB de. 1,3-Propanediol: production, applications and biotechnological potential. Quim Nova [Internet]. 2014;37(3):527–34. Available from: http://www.scielo.br/scielo.php?script=sci_arttext&pid=S0100-40422014000300023&lng=en&nrm=iso&tlng=pt
6. Hao J, Xu F, Liu H, Liu D. Downstream processing of 1,3-propanediol fermentation broth. J Chem Technol Biotechnol. 2006;81(1):102–8.
7. Chatzifragkou A, Aggelis G, Komaitis M, Zeng AP, Papanikolaou S. Impact of anaerobiosis strategy and bioreactor geometry on the biochemical response of Clostridium butyricum VPI 1718 during 1,3-propanediol fermentation. Bioresour Technol [Internet]. 2011;102(22):10625–32. Available from: http://dx.doi.org/10.1016/j.biortech.2011.09.023
8. Murarka A, Dharmadi Y, Yazdani SS, Gonzalez R. Fermentative utilization of glycerol by Escherichia coli and its implications for the production of fuels and chemicals. Appl Environ Microbiol. 2008;74(4):1124–35.
9. Homann T, Tag C, Biebl H, Deckwer WD, Schink B. Fermentation of glycerol to 1,3-propanediol by Klebsiella and Citrobacter strains. Appl Microbiol Biotechnol. 1990;33(2):121–6.
10. Biebl H, Menzel K, Zeng AP, Deckwer WD. Microbial production of 1,3-propanediol. Appl Microbiol Biotechnol. 1999;52(3):289–97.
11. Hong WK, Kim CH, Heo SY, Luo LH, Oh BR, Rairakhwada D, et al. 1,3-Propandiol production by engineered Hansenula polymorpha expressing dha genes from Klebsiella pneumoniae. Bioprocess Biosyst Eng. 2011;
12. Celińska E. Debottlenecking the 1,3-propanediol pathway by metabolic engineering. Vol. 28, Biotechnology Advances. 2010. p. 519–30.
13. Johnson EA, Lin ECC. Klebsiella pneumoniae 1,3-Propanediol:NAD+ Oxidoreductase. J Bacteriol. 1987;169(5):2050–4.
14. Chen X, Zhang DJ, Qi WT, Gao SJ, Xiu ZL, Xu P. Microbial fed-batch production of 1,3-propanediol by Klebsiella pneumoniae under micro-aerobic conditions. Appl Microbiol Biotechnol. 2003;63(2):143–6.
15. Maervoet VET, De Mey M, Beauprez J, De Maeseneire S, Soetaert WK. Enhancing the microbial conversion of glycerol to 1,3-propanediol using metabolic engineering. Org Process Res Dev. 2011;15(1):189–202.
16. Maervoet VET, De Maeseneire SL, Avci FG, Beauprez J, Soetaert WK, De Mey M. High yield 1,3-propanediol production by rational engineering of the 3-hydroxypropionaldehyde bottleneck in Citrobacter werkmanii. Microb Cell Fact. 2016;15(1):1–11.
17. Lu X, Fu X, Zong H, Zhuge B. Overexpressions of xylA and xylB in Klebsiella pneumoniae lead to enhanced 1, 3-propanediol production by cofermentation of glycerol and xylose. J Microbiol Biotechnol. 2016;26(7):1252–8.
18. Lu XY, Ren SL, Lu JZ, Zong H, Song J, Zhuge B. Enhanced 1,3-propanediol production in Klebsiella pneumoniae by a combined strategy of strengthening the TCA cycle and weakening the glucose effect. J Appl Microbiol. 2018;124(3):682–90.
19. Flora AB. Detecção e clonagem de genes de biossíntese de 1,3-propanodiol a partir de glicerol em Klebsiella pneumoniae GLC29. 2015.
20. Oliveira H da C. Impacto da inativação de genes relacionados à síntese de productos de fermentação (lactato e acetato) na produção de 1,3-propanodiol em linhagens de Escherichia coli recombinantes. 2017.
21. Gunsalus RP. Control of electron flow in Escherichia coli: Coordinated transcription of respiratory pathway genes. J Bacteriol. 1992;174(22):7069–74.
22. Zhu J, Shalel-Levanon S, Bennett G, San KY. Effect of the global redox sensing/regulation networks on Escherichia coli and metabolic flux distribution based on C-13 labeling experiments. Metab Eng. 2006;8(6):619–27.
23. Iuchi S. Phosphorylation/dephosphorylation of the receiver module at the conserved aspartate residue controls transphosphorylation activity of histidine kinase in sensor protein ArcB of Escherichia coli. J Biol Chem. 1993;268(32):23972–80.
24. Georgellis D, Kwon O, Lin ECC. Quinones as the redox signal for the Arc two-component system of

bacteria. Science (80-). 2001;292(5525):2314–6.
25. Malpica R, Franco B, Rodriguez C, Kwon O, Georgellis D. Identification of a quinone-sensitive redox switch in the ArcB sensor kinase. Proc Natl Acad Sci U S A. 2004;101(36):13318–23.
26. Drapal N, Sawers G. Purification of ArcA and analysis of is specific interaction with the pfl promoter-regulatory region. Mol Microbiol. 1995;16(3):597–607.
27. Iuchi S, Matsuda Z, Fujiwara T, Lin ECC. The arcB gene of Escherichia coli encodes a sensor-regulator protein for anaerobic repression of the arc modulon. Mol Microbiol. 1990;4(5):715–27.
28. Tseng C, Albrecht J, Gunsalus RP. Effect of Microaerophilic Cell Growth Conditions on Expression.pdf. J Bacteriol. 1996;178(4):1094–8.
29. Shalel-Levanon S, San KY, Bennett GN. Effect of ArcA and FNR on the expression of genes related to the oxygen regulation and the glycolysis pathway in Escherichia coli under microaerobic growth conditions. Biotechnol Bioeng. 2005;92(2):147–59.
30. Rice CW, Hempfling WP. Oxygen-Linmited Continuous Culture and Respiratory Energy.pdf. J Bacteriol. 1978;134(1):115–24.
31. Reddy SG, Wong KK, Parast C V, Peisach J, Magliozzo RS, Kozarich JW. Dioxygen inactivation of pyruvate formate-lyase: EPR evidence for the formation of protein-based sulfinyl and peroxyl radicals. Biochemistry. 1998;37(2):558–63.
32. Alexeeva S, De Kort B, Sawers G, Hellingwerf KJ, De Mattos MJT. Effects of limited aeration and of the ArcAB system on intermediary pyruvate catabolism in Escherichia coli. J Bacteriol. 2000;182(17):4934–40.
33. Shimizu K. Metabolic Regulation of a Bacterial Cell System with Emphasis on Escherichia coli Metabolism. ISRN Biochem. 2013;2013:1–47.
34. Bekker M, Alexeeva S, Laan W, Sawers G, De Mattos JT, Hellingwerf K. The ArcBA two-component system of Escherichia coli is regulated by the redox state of both the ubiquinone and the menaquinone pool. J Bacteriol. 2010;192(3):746–54.
35. Levanon SS, San KY, Bennett GN. Effect of oxygen on the Escherichia coli ArcA and FNR regulation systems and metabolic responses. Biotechnol Bioeng. 2005;89(5):556–64.
36. Unden G, Schirawski J. The oxygen-responsive transcriptional regulator FNR of Escherichia coli: the search for signals and reactions. Mol Microbiol. 1997;25:205–10.
37. Kumar V, Park S. Potential and limitations of Klebsiella pneumoniae as a microbial cell factory utilizing glycerol as the carbon source. Biotechnol Adv [Internet]. 2018;36(1):150–67. Available from: https://doi.org/10.1016/j.biotechadv.2017.10.004
38. Tong IT, Liao HH, Cameron DC. 1,3-Propanediol production by Escherichia coli expressing genes from the Klebsiella pneumoniae dha regulon. Appl Environ Microbiol. 1991;
39. Liang Q, Zhang H, Li S, Qi Q. Construction of stress-induced metabolic pathway from glucose to 1,3-propanediol in Escherichia coli. Appl Microbiol Biotechnol. 2011;
40. Przystałowska H, Lipiński D, Słomski R. Biotechnological conversion of glycerol from biofuels to 1 , 3-propanediol using Escherichia coli. Acta Biochim Pol [Internet]. 2015;62(1):23–34. Available from: file:///C:/Users/Hendor Neves/Downloads/Biotechnological conversion - Acta Biochimica Polonica.pdf
41. Tang X, Tan Y, Zhu H, Zhao K, Shen W. Microbial conversion of glycerol to 1,3-propanediol by an engineered strain of escherichia coli. Appl Environ Microbiol. 2009;75(6):1628–34.
42. Seo JW, Seo MY, Oh BR, Heo SY, Baek JO, Rairakhwada D, et al. Identification and utilization of a 1,3-propanediol oxidoreductase isoenzyme for production of 1,3-propanediol from glycerol in Klebsiella pneumoniae. Appl Microbiol Biotechnol. 2010;85(3):659–66.
43. Ferrer-Miralles N, Domingo-Espín J, Corchero J, Vázquez E, Villaverde A. Microbial factories for recombinant pharmaceuticals. Microb Cell Fact. 2009;8:1–8.
44. Sodoyer R, Courtois V, Peubez I, Migno C. Antibiotic-Free Selection for Bio-Production: Moving Towards a New “Gold Standard.” Antibiot Resist Bact - A Contin Chall New Millenn. 2012;
45. Cranenburgh RM. Escherichia coli strains that allow antibiotic-free plasmid selection and maintenance by repressor titration. Nucleic Acids Res. 2001;29(5):26e – 26.
46. Abeles AL, Friedman SA, Austin SJ. Partition of unit-copy miniplasmids to daughter cells. III. The DNA sequence and functional organization of the P1 partition region. J Mol Biol. 1985;185(2):261–72.
47. Kaur T, Al Abdallah Q, Nafissi N, Wettig S, Funnell BE, Slavcev RA. ParAB-mediated intermolecular association of plasmid P1 parS Sites. Virology. 2011;421(2):192–201.
48. Hernández-arriaga ANAM, Chan WAIT, Espinosa M, Díaz-orejas R. Conditional Activation of Toxin-Antitoxin Systems: Postsegregational Killing and Beyond. Plasmids Biol Impact Biotechnol Discov. 2015;175–92.
49. Loison. © 19 8 6 Nature Publishing Group http://www.nature.com/naturebiotechnology. Nat Biotechnol. 1986;4(August):719–25.
50. Velur Selvamani RS, Telaar M, Friehs K, Flaschel E. Antibiotic-free segregational plasmid stabilization in Escherichia coli owing to the knockout of triosephosphate isomerase (tpiA). Microb Cell Fact. 2014;13(1):1–13.
51. Zhu K, Li G, Wei R, Mao Y, Zhao Y, He A, et al. Systematic analysis of the effects of different nitrogen source and ICDH knockout on glycolate synthesis in Escherichia coli. J Biol Eng. 2019;13(1):1–13.
52. Anderson J. Anderson promoter collection [Internet]. Available from: http://parts.igem.org/Promoters/Catalog/Anderson
53. Datsenko KA, Wanner BL. One-step inactivation of chromosomal genes in Escherichia coli K-12 using

PCR products. Proc Natl Acad Sci U S A [Internet]. 2000;97(12):6640–5. Available from: http://www.pubmedcentral.nih.gov/articlerender.fcgi?artid=18686&tool=pmcentrez&rendertype=abstract
54. Schimidell W, Lima U de A, Aquarona E, Borzani W. Biotecnologia Industrial. Vol. 2. 2001. 282 p.
55. Kotrola JS. Growth and survival of Escherichia coli O157 : H7 under acidic conditions . These include : Growth and Survival of Escherichia coli O157 : H7 under Acidic Conditions †. Appl Environ Microbiol. 1995;61(1):7–11.
56. Canonaco F, Hess TA, Heri S, Wang T, Szyperski T, Sauer U. Metabolic flux response to phosphoglucose isomerase knock-out in Escherichia coli and impact of overexpression of the soluble transhydrogenase UdhA. FEMS Microbiol Lett. 2001;204(2):247–52.
57. Zablotny R, Fraenkel DG. Glucose and gluconate metabolism in a mutant of Escherichia coli lacking gluconate-6-phosphate dehydrase. J Bacteriol. 1967;93(5):1579–81.
58. Lim SJ, Jung YM, Shin HD, Lee YH. Amplification of the NADPH-related genes zwf and gnd for the oddball biosynthesis of PHB in an E. coli transformant harboring a cloned phbCAB operon. J Biosci Bioeng. 2002;93(6):543–9.
59. Sauer U, Canonaco F, Heri S, Perrenoud A, Fischer E. The Soluble and Membrane-bound Transhydrogenases UdhA and PntAB Have Divergent Functions in NADPH Metabolism of Escherichia coli. J Biol Chem. 2004;279(8):6613–9.
60. Lynch S, Eckert C, Yu J, Gill R, Maness PC. Overcoming substrate limitations for improved production of ethylene in E. coli. Biotechnol Biofuels. 2016;9(1):1–10.
61. Perez-Zabaleta M, Sjöberg G, Guevara-Martínez M, Jarmander J, Gustavsson M, Quillaguamán J, et al. Increasing the production of (R)-3-hydroxybutyrate in recombinant Escherichia coli by improved cofactor supply. Microb Cell Fact. 2016;15(1):1–10.
62. Siegel WH, Donohue T, Bernlohr RW. Determination of pools of tricarboxylic acid cycle and related acids in bacteria. Appl Environ Microbiol. 1977;34(5):512–7.
63. Yan D, Lenz P, Hwa T. Overcoming fluctuation and leakage problems in the quantification of intracellular 2-oxoglutarate levels in Escherichia coli. Appl Environ Microbiol. 2011;77(19):6763–71.
64. Seol W, Shatkin AJ. Escherichia coli kgtP encodes an α-ketoglutarate transporter. Proc Natl Acad Sci U S A. 1991;88(9):3802–6.
65. Cai W, Cai X, Yang Y, Yan S, Zhang H. Transcriptional control of dual transporters involved in α-ketoglutarate utilization reveals their distinct roles in uropathogenic escherichia coli. Front Microbiol. 2017;8(FEB):1–14.
66. Barroca M, Rodrigues P, Sobral R, Costa MMR, Chaves SR, MacHado R, et al. Antibiotic free selection for the high level biosynthesis of a silk-elastin-like protein. Sci Rep. 2016;6(July):1–11.
67. Sánchez AM, Bennett GN, San KY. Effect of different levels of NADH availability on metabolic fluxes of Escherichia coli chemostat cultures in defined medium. J Biotechnol. 2005;117(4):395–405.
68. Berríos-Rivera SJ, Bennett GN, San KY. Metabolic engineering of Escherichia coli: Increase of NADH availability by overexpressing an NAD+-dependent formate dehydrogenase. Metab Eng. 2002;4(3):217–29.
69. Berríos-Rivera SJ, Bennett GN, San KY. The effect of increasing NADH availability on the redistribution of metabolic fluxes in Escherichia coli chemostat cultures. Metab Eng. 2002;4(3):230–7.
70. Mark R. The Steady-State Internal Redox State (NADH / NAD) Reflects the External Redox State and Is Correlated with Catabolic Adaptation in Escherichia coli. 1999;181(8):2351–7.
71. Bernal V, Castaño-Cerezo S, Cánovas M. Acetate metabolism regulation in Escherichia coli: carbon overflow, pathogenicity, and beyond. Appl Microbiol Biotechnol [Internet]. 2016;100(21):8985–9001. Available from: http://dx.doi.org/10.1007/s00253-016-7832-x
72. Shalel-Levanon S, San KY, Bennett GN. Effect of oxygen, and ArcA and FNR regulators on the expression of genes related to the electron transfer chain and the TCA cycle in Escherichia coli. Metab Eng. 2005;7(5–6):364–74.

*De acordo com: International Committee of Medical Journal Editors. Uniform requirements for manuscripts submitted to Biomedical Journal: sample references. 2003 [cited 2016 May 30]. Available from: https://www.nlm.nih.gov/bsd/uniform_requirements.html

APPENDIX A – pBBR1MCS2::*dha* production plasmid map

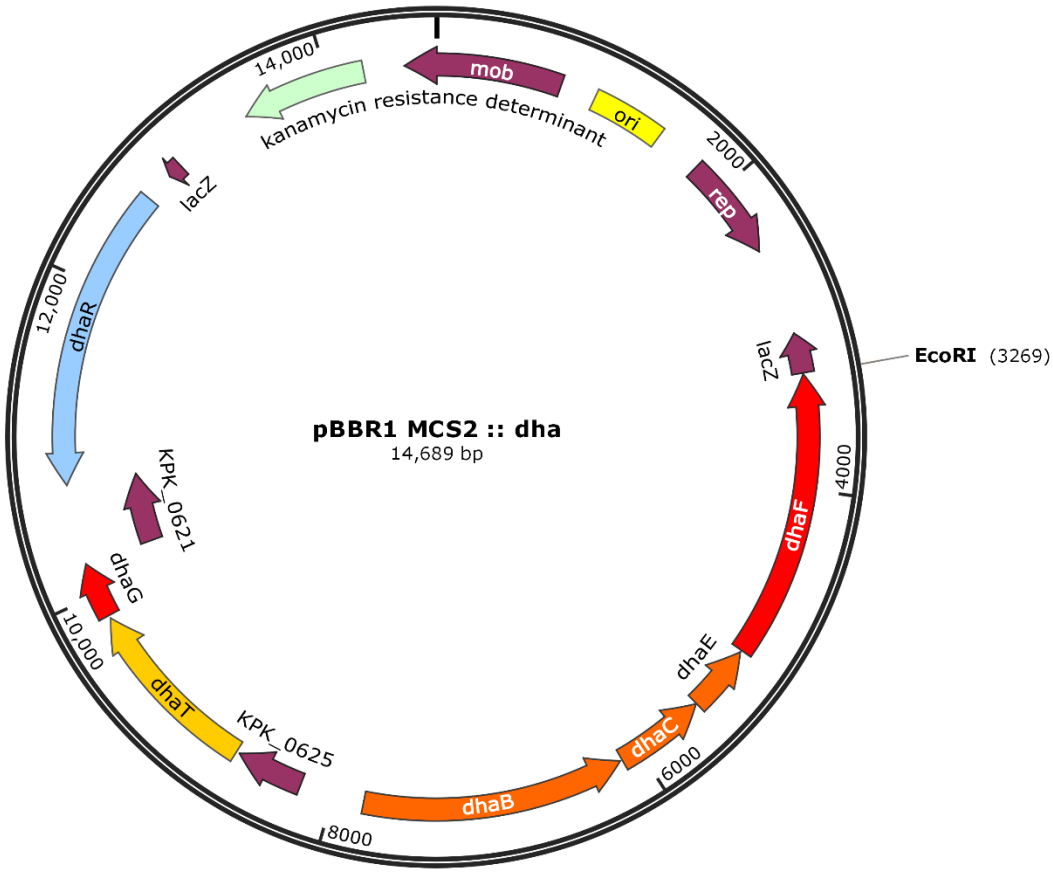

Schematic representation of pBBR1MCS2 :: *dha* production plasmid. *EcoRI* restriction site was used to insert the *icd* gene in the vector.

APPENDIX B – icdNADP strain plasmid stability assay

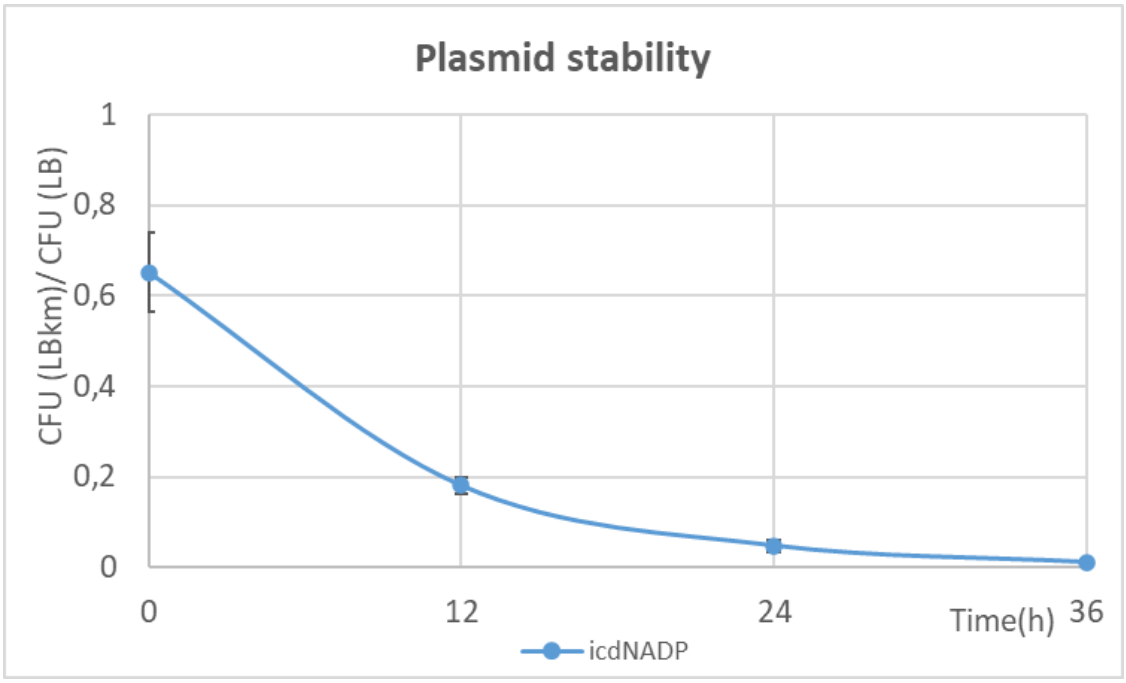

Shake flask assay in Mineral medium comparing the stability of plasmids carried by bacteria. The stability was calculated by the fraction of numbers of colonies that grew in LB with Kanamycin and in LB without antibiotic ($CFU^{LB\ Km}$/ CFU^{LB}). The experiment was performed in three replicates using icdNADP strain; the bar shows the standard error.

APPENDIX C – Pyruvate and acetate accumulation after anti-foam addition.

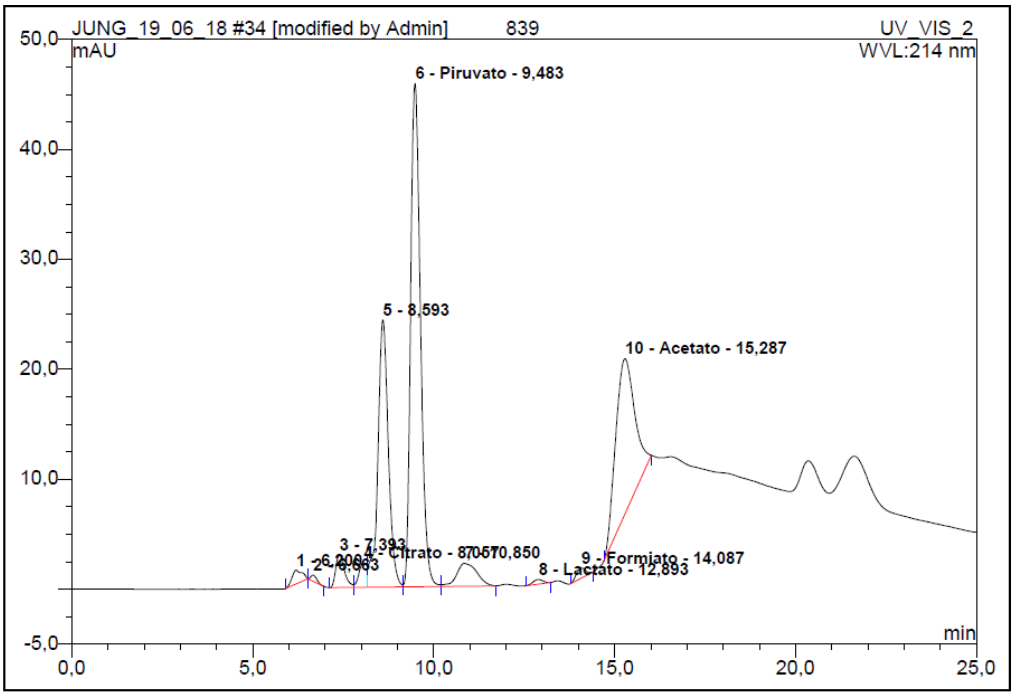

Organic acids detected through HPLC. This pattern repeats in all bioreactors that failed after the addition of anti-foam. Peak number 6: pyruvate; peak number 10: acetate.